Relaxation time for competing short- and long-range interactions in the model A dynamic universality class

Jean-François de Kemmeter, 1,2 Stefano Ruffo, 3,4 and Stefano Gherardini 1

¹Istituto Nazionale di Ottica del Consiglio Nazionale delle Ricerche (CNR-INO), Largo Enrico Fermi 6, I-50125 Firenze, Italy.

²Department of Mathematics, Royal Military Academy, Brussels, Belgium.

³Istituto dei Sistemi Complessi del Consiglio Nazionale delle Ricerche (CNR-ISC),

Via Madonna del Piano 10, I-50019 Sesto Fiorentino, Italy.

⁴INFN, Sezione di Firenze, I-50019 Sesto Fiorentino, Italy.

We study the relaxation dynamics at criticality in the one-dimensional spin-1/2 Nagle-Kardar model, where short- and long-range interactions can compete. The phase diagram of this model shows lines of first and second-order phase transitions, separated by a tricritical point. We consider Glauber dynamics, focusing on the slowing-down of the magnetization m both along the critical line and at the tricritical point. Starting from the master equation and performing a coarse-graining procedure, we obtain a Fokker-Planck equation for m and the fraction of defects. Using central manifold theory, we analytically show that m decays asymptotically as $t^{-1/2}$ along the critical line, and as $t^{-1/4}$ at the tricritical point. This result implies that the dynamical critical exponent is z=2, proving that the macroscopic critical dynamics of the Nagle-Kardar model falls within the dynamic universality class of purely relaxational dynamics with a non-conserved order parameter (model A). Large deviation techniques enable us to show that the average first passage time between local equilibrium states follows an Arrhenius law.

Long-range classical and quantum interacting systems [1–4] are characterized by an inter-particle potential V(r) that decays as $V(r) \sim r^{-\alpha}$ at large separation r. Examples include Coulomb interactions [5], self-gravitating systems [6], two-dimensional turbulence [7], and recently Riesz gases [8, 9].

In many real-world systems short- and long-range interactions coexist and can compete. The addition of a mean-field term to the Ising Hamiltonian was first proposed by Baker [10] and later analyzed in the canonical ensemble by Nagle [11] and Kardar [12]. In the phase diagram of this model there are lines of first and second-order phase transitions separated by a tricritical point [13]. The Nagle-Kardar model can represent such diverse physical systems as: bond percolation in the presence of infinite-range bonds [14], spin systems on small-world hypergraphs [15], single-chain magnets [16], synchronization with long-range interactions [17], and bosons in an optical lattice with cavity-induced long-range interactions [18]. Recently, the Nagle-Kardar model has been used to characterize finite-size effects, like the Casimir force, near criticality [19-21], and the addition of next-to-nearest neighbor and biquadratic interactions has been also considered [22–24].

While the static properties of the Nagle-Kardar model have been widely studied, dynamical properties have not been addressed carefully, if we exclude a single paper where simulations of the dynamics in the microcanonical ensemble are performed [13]. On the other hand, critical slowing down, bistability and metastability have been investigated for the Ising [25–27] and the Curie-Weiss [28–30] models separately.

In this Letter, we study the dynamics of the onedimensional Nagle-Kardar model in the canonical ensemble, using numerical simulations and analytical tools. Our main contributions are: *i*) the derivation of a Fokker-Planck equation from the microscopic Glauber dynamics [31]; *ii*) the analytical determination of the dynamical critical exponent z that governs the algebraic slowing-down of the magnetization along the second-order critical line and at the tricritical point.

We begin with the exact master equation that represents the stochastic evolution of the spin configurations under Glauber dynamics [32, 33]. In order to reduce the system dimensionality, we perform a coarse-graining procedure by classifying the configurations in terms of two macroscopic variables: the total magnetization M and the number of defects 2S that separate adjacent, oppositely aligned spins [34]. Then, we derive the master equation that describes the time evolution of the joint probability distribution $P_N(M, 2S; t)$, where N is the system size. In the large-N limit, we obtain the Fokker-Planck equation for the time evolution of the joint probability distribution p(m, s; t) in terms of the intensive variables $m = M/N \in [-1, 1]$ and s = 2S/N.

From the Fokker-Planck equation, we determine the asymptotic dynamics of the magnetization m. Based on considerations from scaling theory [27, 35–38], the average absolute magnetization is expected to decay algebraically at criticality, both in time and with respect to N:

$$\langle |m(t)| \rangle \sim t^{-\lambda_m}$$
 and $\langle |m| \rangle \sim N^{-\Delta_m}$, (1)

where the latter holds at equilibrium. We derive analytically that $\lambda_m = 1/2$ along the critical line, and $\lambda_m = 1/4$ at the tricritical point. The exponent λ_m is related to the static exponents β , ν and to the dynamical exponent z by the relation $\lambda_m = \beta/(z\nu)$ [27]. We show that this implies z = 2, which is the dynamical critical exponent of the model A dynamic universality class [25]. Model A describes Markovian critical dynamical phenomena with non-conserved order parameter. Moreover, $\Delta_m = 1/4$ for the critical line [29, 39], and $\Delta_m = 1/6$ at the tricritical point. This result follows from

$$\Delta_m = \frac{\beta}{\nu \, d_u},\tag{2}$$

where d_u is the upper critical dimension [40]. We show the validity of Eq. (2) for systems where short- and long-range

interactions compete, thus extending its application beyond short-range interaction systems. In our analysis, we get $d_u = 4$ on the critical line, and $d_u = 3$ at the tricritical point.

Finally, we study bistable and metastable states in the Nagle-Kardar model, finding that the average transition time follows an Arrhenius law, with exponential scaling in *N*, similarly with results valid for long-range interactions [13, 41–43].

The Nagle-Kardar model: equilibrium properties.—We consider a one-dimensional periodic chain of N spins $s_i \in \{\pm 1\}$, described by the Hamiltonian

$$H = -J \sum_{i=1}^{N} s_i s_{i+1} - \frac{K}{2N} \left(\sum_{i=1}^{N} s_i \right)^2 - h \sum_{i=1}^{N} s_i,$$
 (3)

where J, K are the nearest-neighbor and mean-field coupling respectively, and h denotes the external field. Periodic boundary conditions imply $s_{N+1} = s_1$. The total magnetization of the chain is defined as $M = \sum_{i=1}^{N} s_i$, while the (even) number of defects is $2S = \sum_{i=1}^{N} (1 - s_i s_{i+1})/2$. Using M and S, Hamiltonian (3) can be rewritten as $H = -J(N-4S) - \frac{K}{2N}M^2 - hM$.

The phase diagram of the Nagle-Kardar model in the plane h=0 exhibits a tricritical point at $J/T=-\log(3)/4$ and $K/T=\sqrt{3}$ [11, 12], where T is the temperature with k_B set to 1. At the tricritical point, a line of second-order phase transition meets a line of first-order transitions, see Supplemental Material (SM) [44]. Explicit computations (fully detailed in the SM) show that, at equilibrium, the joint probability distribution $P_N(M,2S)$ satisfies the large-deviation principle [45] in the large-N limit:

$$P_N(M,2S) \approx e^{-NU(m,s)},\tag{4}$$

where \times means that $U(m, s) = -\lim_{N \to +\infty} \log (P_N(M, 2S))/N$. Here, U(m, s) is a non-negative quasi-potential given by

$$U(m, s) = s \log(s) - \frac{1+m}{2} \log(1+m) - \frac{1-m}{2} \log(1-m) + \frac{1+m-s}{2} \log(1+m-s) + \frac{1-m-s}{2} \log(1-m-s) + \frac{1}{T} \left(\frac{K}{2}m^2 + hm + J(1-2s) + f\right),$$
 (5)

where f denotes the system free-energy. The defect density s satisfies $0 \le s \le 1 - |m|$ [46].

In Fig. 1 we plot the potential U(m, s) for h = 0; in absence of the external field the potential is symmetric in m. As $N \to +\infty$, the equilibrium values of the magnetization per site m^* and fraction of defects s^* are determined by the condition $U(m^*, s^*) = 0$. As detailed in the SM, m^* satisfies the following implicit equation [20]

$$m^* = \frac{\sinh((h + Km^*)/T)}{\sqrt{\sinh^2((h + Km^*)/T) + e^{-4J/T}}}.$$
 (6)

Instead, the fraction of defects s^* depends on m^*

$$s^* = \frac{1 - \sqrt{m^{*2} + e^{4J/T}(1 - m^{*2})}}{1 - e^{4J/T}}.$$
 (7)

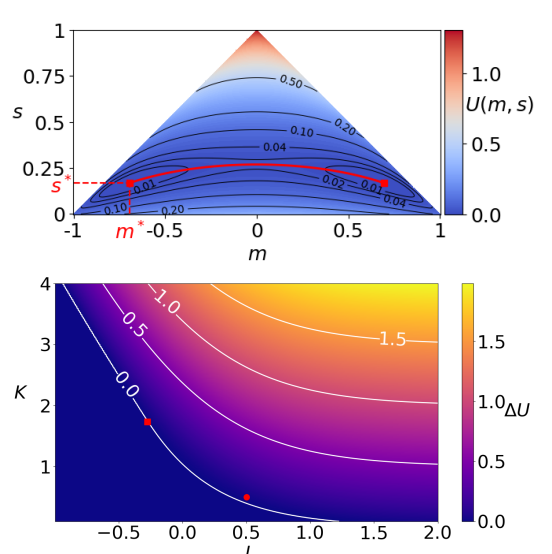


FIG. 1: (Top) Quasi-potential U(m, s) with parameters T=1, h=0, J=1/2 and K=1/2. The two minima (m^*, s^*) , such that $U(m^*, s^*)=0$, are highlighted by the red squares. A few contour lines are shown in black. The red curve represents the solution of Eq. (7). (Bottom) Potential barrier ΔU for h=0, separating the two local minima of U(m, s), plotted as a function of J and K, together with a few contour lines. The red point (J=K=0.5) corresponds to the parameter set of the top panel $(\Delta U\approx 0.018)$, while the red square (where $\Delta U=0$) is the tricritical point $(J=-\frac{\log(3)}{4},K=\sqrt{3})$. The contour line $\Delta U=0$ denotes the second-order phase transition for $K<\sqrt{3}$ and the first-order one for $K>\sqrt{3}$.

In the strongly antiferromagnetic limit $J \to -\infty$, the spin system favors the perfectly alternating spin configuration, corresponding to $s^* = 1$. In contrast, when $J/T \to 0$, the magnetization per site is $m^* = \tanh((h + Km^*)/T)$ and $s^* \approx \frac{1-m^{*2}}{2}$.

The probability distribution of the magnetization, $P_N(M)$, can be obtained by taking the marginal of the distribution $P_N(M, 2S)$. One obtains (see SM): $P_N(M) \times e^{-N\psi(m)}$, where

$$\psi(m) = -\frac{1}{T} \left(J - hm - \frac{K}{2} m^2 - f \right) - \frac{1+m}{2} \log \left(1 - \frac{1}{\xi(m)} \right) + -\frac{1-m}{2} \log \left(1 - e^{-4J/T} \xi(m) \right),$$
(8)

with $\xi(m) = -\frac{m}{1-m} - \frac{1}{1-m} \sqrt{m^2 + e^{4J/T}(1-m^2)}$. The function $\psi(m)$, shown in the End Matter (EM), is non-negative and vanishes at $m=m^*$. From Eq. (8) we deduce that $|m^*| \sim N^{-1/2}$ in the disordered phase and away from the second-order transition line, while $|m^*| \sim N^{-1/4}$ at the second-order line $K/T = e^{-2J/T}$, except at the tricritical point where $|m^*| \sim N^{-1/6}$. We recover the results of [47] in the limiting cases of the one-dimensional Ising (K=0) and Curie-Weiss (L=0) models.

Dynamics: Master equation for the Glauber dynamics.— We explore the time evolution of spin configurations using the Glauber dynamics [48]. Starting from a configuration σ , a spin is selected uniformly at random and flipped with acceptance probability $1/(1+e^{\Delta E/T})$, where ΔE is the energy change associated with the flip of the selected spin. The probability $\mathbb{P}(\sigma;t)$ to observe a configuration σ at time t is ruled by the master equation

$$\frac{d\mathbb{P}(\boldsymbol{\sigma};t)}{dt} = \sum_{\boldsymbol{\sigma}'} \left[\mathbf{T}_{\boldsymbol{\sigma}\boldsymbol{\sigma}'} \mathbb{P}(\boldsymbol{\sigma}';t) - \mathbf{T}_{\boldsymbol{\sigma}'\boldsymbol{\sigma}} \mathbb{P}(\boldsymbol{\sigma};t) \right], \tag{9}$$

where $T_{\sigma\sigma'}$ is the Markovian transition rate for passing from the configuration σ' to the configuration σ . These rates form the entries of a $2^N \times 2^N$ transition matrix. In order to reduce the complexity of the dynamics, we adopt a coarse-grained description of the configurations, whose dynamics is governed by the joint probability distribution $P_N(M, 2S; t)$ in terms of M and 2S (see the formal derivation in the SM).

To derive the time evolution of $P_N(M, 2S; t)$ we analyze how single spin flips affect the macroscopic variables M and 2S. Given a spin configuration σ with magnetization M and 2S defects, flipping a single spin results in a new configuration σ' with updated magnetization $M' \in \{M \pm 2\}$ and number of defects $2S' \in \{2S, 2S \pm 2\}$. The corresponding dynamics is described by the master equation

$$\frac{dP_N(M,2S;t)}{dt} = -\sum_{\substack{\Delta M = \pm 2 \\ \Delta S = 0, \pm 2}} \mathcal{T}(M + \Delta M, 2S + \Delta S | M, 2S) P_N(M, 2S;t)$$
broadening of the Dirac δ solution. From the Fokker-Planck equation SM) the associated Langevin equation

+
$$\sum_{\substack{\Delta M = \pm 2 \\ \Delta S = 0, \pm 2}} \mathcal{T}(M, 2S | M + \Delta M, 2S + \Delta S) P_N(M + \Delta M, 2S + \Delta S; t)$$
. (10) for $X = (m, s)^{\text{tr}}$ ('tr' denotes transposition):

The transition rates \mathcal{T} are products of two factors: (i) the probability of choosing a specific spin within a configuration and (ii) the Glauber transition probabilities. While the latter factor depends only on the energy change and, hence, only on the change in M and S, the first factor depends, a priori, on all specific features of the configurations. In the SM, we show that, under reasonable hypotheses, also such factor depends only on M and S. In order to illustrate the validity of this coarse-graining procedure, in the EM, the exact Glauber dynamics is compared with the coarse-grained one, observing an excellent agreement even for small sizes.

Dynamics: Fokker-Planck and Langevin equations.—We now assume N to be large, and we expand the master equation (10) in powers of $\epsilon = 1/N$ (see Section VIII of [49]). At first order in ϵ , we obtain an associated Fokker-Planck equation that describes the time evolution of the rescaled probability density $p(m, s; t) = \lim_{N \to +\infty} \frac{N^2}{4} P_N(M = mN, 2S = sN; tN)$ [50]. Here, the time has been rescaled and is expressed in units of Monte Carlo sweeps. After some computations, shown in the SM, we derive that

$$\frac{\partial p(m, s; t)}{\partial t} = \frac{\partial}{\partial m} [D_1(m, s)p(m, s; t)] + \frac{\partial}{\partial s} [D_2(m, s)p(m, s; t)]
+ \epsilon \frac{\partial^2}{\partial m^2} [D_{mm}(m, s)p(m, s; t)] + \epsilon \frac{\partial^2}{\partial s^2} [D_{ss}(m, s)p(m, s; t)]
+ 2\epsilon \frac{\partial^2}{\partial m \partial \sigma} [D_{ms}(m, s)p(m, s; t)],$$
(11)

where the drift coefficients are

$$D_{1}(m,s) = m + c_{1} \tanh(x) + c_{2} \tanh(x_{-}) + c_{3} \tanh(x_{+}) + K\epsilon \left(\frac{c_{4}}{\cosh^{2}(x)} + \frac{c_{5}}{\cosh^{2}(x_{-})} + \frac{c_{6}}{\cosh^{2}(x_{+})}\right),$$

$$D_{2}(m,s) = 2s - 1 + c_{2} \tanh(x_{-}) - c_{3} \tanh(x_{+}) + K\epsilon \left(\frac{c_{5}}{\cosh^{2}(x_{-})} - \frac{c_{6}}{\cosh^{2}(x_{+})}\right), \tag{12}$$

while the diffusion coefficients are defined as

$$D_{mm}(m, s) = 1 - c_4 \tanh(x) - c_5 \tanh(x_-) - c_6 \tanh(x_+),$$

$$D_{ss}(m, s) = 1 + c_1 - c_5 \tanh(x_-) - c_6 \tanh(x_+),$$

$$D_{ms}(m, s) = -m - c_5 \tanh(x_-) + c_6 \tanh(x_+)$$
(13)

with x = h + Km and $x_{\pm} = x \pm 2J$ (T = 1). The drift and diffusion coefficients $c_i = c_i(m, s)$, reported in the SM, are all functions of m and s. The correctness of our results is confirmed by taking J = 0, corresponding to the Curie-Weiss model. In this case, indeed, we recover the expression derived in [51]. In the $\epsilon = 0$ case, the stationary solution of Eq. (11) is $p(m, s) = \delta(m - m^*)\delta(s - s^*)$, where m^* and s^* are given in Eqs. (6)-(7). The effect of having a finite value of ϵ is the broadening of the Dirac δ solution.

From the Fokker-Planck equation (11), one can obtain (see SM) the associated Langevin equation for the stochastic vector $X = (m, s)^{tr}$ ('tr' denotes transposition):

$$dX_t = D(X_t)dt + \sqrt{2\epsilon} B(X_t) dW_t, \qquad (14)$$

where $D(X) = -(D_1(m, s), D_2(m, s))^{tr}$ is the drift, W_t is a standard Brownian motion and B is the 2×2 diffusion matrix

$$\begin{pmatrix} \sqrt{D_{mm}} & 0\\ \frac{D_{ms}}{\sqrt{D_{mn}}} & \sqrt{D_{ss} - \frac{D_{ms}^2}{D_{mm}}} \end{pmatrix}. \tag{15}$$

Dynamics: Universal slowing down at both the critical line and the tricritical point.—Dynamical scaling theory [25, 27, 35–38] allows us to formulate the following finite-size scaling relation for the average absolute magnetization $\langle |m(t, N)| \rangle$:

$$\langle |m(t,N)| \rangle \sim N^{-\Delta_m} g\left(t N^{-\frac{\Delta_m}{\lambda_m}}\right),$$
 (16)

where *g* is a model-dependent function [52]. From (16), we obtain the scaling formulas (1), by imposing $t \sim N^{z/d_u}$ [25].

On the critical line, it is known that the static critical exponents are those of the mean-field theory [53], i.e., $\beta = 1/2$ and $\nu = 1/2$ [54]. To determine Δ_m in Eq. (2), one has to fix a value of d_u . Following [29, 39], we guess that the mean-field term in the Nagle-Kardar model dominates the critical phenomena, such that one can set $d_u = 4$. The ensuing value of $\Delta_m = 1/4$ is obtained from Eq. (2). It coincides with the value that we compute by scaling the probability of magnetization with N, using the large-deviation function $\psi(m)$ of Eq. (8). This result is confirmed numerically by looking at the scaling of $\langle |m(t, N)| \rangle$ with N at large t; see the inset of Fig. 2 at left.

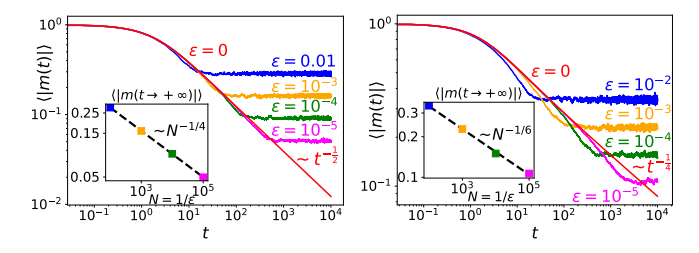


FIG. 2: (Left) Time evolution of $\langle |m(t,N)| \rangle$, in log-log scale, at the critical point of the Curie-Weiss model, for decreasing values of $\epsilon=1/N$. We find that z=2 in an intermediate time range, before the magnetization reaches the equilibrium plateau proportional to $N^{-1/4}$ (see inset). (Right) Time evolution of $\langle |m(t,N)| \rangle$, in log-log scale, at the tricritical point of the Nagle-Kardar model [Eq. (3)]. Also for this model z=2, and the asymptotic magnetization fluctuates around $N^{-1/6}$. In all simulations, the average is performed over 1000 independent trajectories, with m(0)=1.

At the tricritical point, using again Eq. (6) for m close to zero, we find that $\beta = 1/4$ (see also SM). We know that the value of ν remains 1/2 because it is related only to the coefficient multiplying the quadratic term in the Landau free-energy [53]. Instead, the upper critical dimension changes to $d_u = 3$ [40], as given by the Ginzburg criterion reported in the EM. Therefore, $\Delta_m = 1/6$ as also confirmed numerically by looking at the large time behavior of $\langle |m(t, N)| \rangle$; see the inset of Fig. 2, right panel. It is remarkable to observe that a similar change of the finite-size exponents from critical to tricritical also holds for the amplitude of the Casimir force [20].

Let us now discuss the value of the dynamical critical exponent z. First, we consider J/T=0 and K/T=1, which corresponds to the critical point of the Curie-Weiss model [51]. In such a case, the time evolution of m around the criticality follows the equation $\frac{dm}{dt} = m - \tanh(Km/T)$, whose integration at K/T=1 entails $m(t) \sim t^{-1/2}$ at large times. This gives $\lambda_m=1/2$, which implies z=2. We show this scaling in Fig. 2 (left panel), where we plot the time evolution of $\langle |m(t,N)| \rangle$ for the Curie-Weiss model, using the Langevin equation (14).

We have extended this analysis of z to the Nagle-Kardar model. Using the center manifold theory [55], we derive the nonlinear evolution equation for m around criticality in the m-direction (see EM):

$$\frac{dm}{dt} = \frac{K^2(K^2 - 3)}{3(1 + K^2)}m^3 + O(m^5). \tag{17}$$

Eq. (17) entails that $\lambda_m = 1/2$ on the critical line, except at the tricritical point where the coefficient in front of m^3 vanishes. Hence, as the coefficient of m^5 is non-zero, $\lambda_m = 1/4$ such that z = 2. We have numerically verified it in Fig. 2 (right panel).

Bistability & Metastability.—Bistable and metastable dynamics, which origin for zero and non-zero external field respectively, are present in the Curie-Weiss model below the transition temperature [28]. It is known that the average first passage time $\langle \tau \rangle$ to the stable state increases exponentially

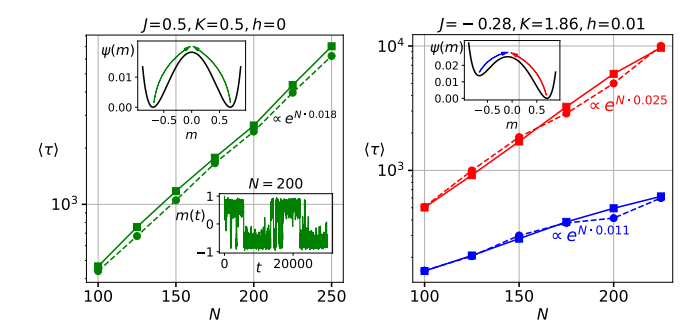


FIG. 3: (Left) Average first passage time $\langle \tau \rangle$ versus N, for h = 0, J = 0.5, K = 0.5 (T = 1) in the Nagle-Kardar model. Zero external field entails bistability. We compare the Glauber (green squares) and Langevin (green dots) dynamics, obtaining a very good agreement. The plot is in semilog scale to highlight the exponential growth with N, and the lines are drawn to guide the eyes. To depict the transitions (green arrows), we report in the upper-left inset the large deviation function $\psi(m)$ [Eq. (8)]. Due to the symmetry of $\psi(m)$, the left-right passage time equals the right-left one. Using Eq. (5), the exponential growth rate is determined by the variation $\Delta U = 0.018$, calculated between the stable and the saddle points in the (m, s) plane. In the lower-right inset, we plot the time-dependence of the magnetization for N = 200, using the Glauber dynamics. (Right) We repeat the same analysis with non-zero h to study metastability, with h = 0.01, J = -0.28, K = 1.86. In this case, $\psi(m)$ is asymmetric (see the inset) and we need to compute two different scaling for the leftright (blue lines) and right-left (red lines) passage times. Here, the rates of exponential increase hold $\Delta U = 0.011$ (blue) and $\Delta U = 0.025$ (red), respectively.

with the system size N [51]. Here, since we derived the Fokker-Planck and Langevin equations for the Nagle-Kardar model [Eqs. (11)-(14)], we analyze bistability and metastability in the ordered phase of such a model.

Fig. 3 displays $\langle \tau \rangle$ as a function of N. We compare Glauber [Eq. (9)] with Langevin [Eq. (14)] dynamics with h=0 (left panel) and $h \neq 0$ (right panel). Using Ref. [56], we derive that $\langle \tau \rangle$ obtained from the Langevin dynamics follows the Arrhenius law

$$\langle \tau \rangle \propto e^{N\Delta U},$$
 (18)

where ΔU denotes the height of the barrier separating the two minima of U(m, s) [Eq. (5)]. Under ergodicity assumptions, the Glauber dynamics gives the same Arrhenius law than the one from Langevin dynamics, as we confirmed numerically [57].

Conclusions.—In this Letter, we analyze the Glauber dynamics within the Nagle-Kardar model. Our main goal was the derivation of the critical exponents that govern the relaxation of the average absolute magnetization $\langle |m(t,N)| \rangle$, starting from a purely microscopic approach. We have determined the value of the critical exponents entering both the relaxation

scaling laws of Eq. (1), using the center manifold theory. In particular, we find that $\lambda_m = 1/2$ and $\Delta_m = 1/4$ on the critical line, while $\lambda_m = 1/4$ and $\Delta_m = 1/6$ at the tricritical point. These exponents result in a dynamical critical exponent of z=2, thus proving that the Nagle-Kardar model belongs to the dynamic universality class of model A. Finally, we have also assessed the exponential scaling of the average first passage time $\langle \tau \rangle$ with the system size, extending a previous result valid for systems with long-range interactions [13].

We expect the Nagle-Kardar model, by incorporating nearest-neighbor interaction effects beyond the mean-field, to enable the study of competing interactions in spin-glass models [58]. The model can then be applied to fields such as atoms in cavity [18], magnetic chains [16], and synchronization [17]. In an interdisciplinary perspective, the Nagle-Kardar model might be also used to determine how nearest-neighbor interactions can enter the modeling of cooperativity phenomena in several fields of chemistry and biology, where only the Curie-Weiss model has been used (e.g. muscle contraction [59] and chemical kinetics [60]).

Acknowledgments.—We acknowledge financial support from the PRIN 2022 PNRR P2022XPT32 "Regulation of striated muscle: a research bridging single molecule to organ (ReStriMus)" funded by the European Union—Next Generation EU, and from the MUR PRIN2022 project BECQuMB Grant No. 20222BHC9Z.

END MATTER

Comparison between Glauber and coarse-grained dynamics

Fig. 4 compares the time evolution of the probability distribution $P_M(t)$ obtained via Glauber dynamics (dots) with the results from the coarse-grained dynamics of $P_N(M, 2S; t)$ (solid lines). Even for small system sizes (N = 7), the agreement is highly satisfactory.

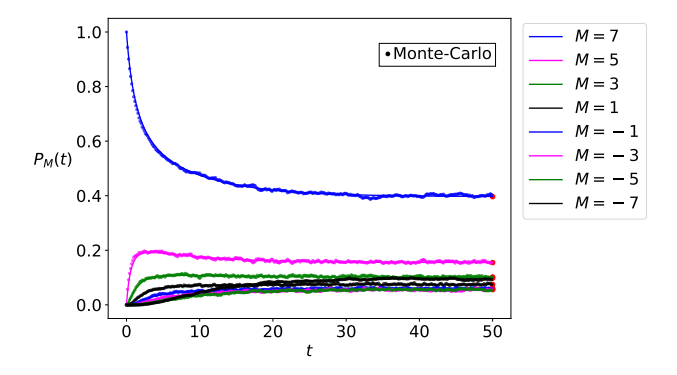


FIG. 4: Comparison between the Glauber dynamics (points) and the coarse-grained dynamics (solid lines) given in Section III in the SM, for the parameters N = 7, T = 1, h = 0.1, J = 0.5 and K = 0.4. Both positive and negative values of M are considered. The points and lines sometimes overlap so perfectly that they are difficult to distinguish.

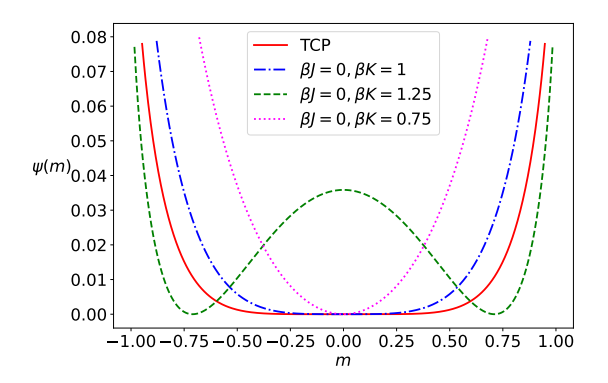


FIG. 5: Large deviation function $\psi(m)$ for several sets of parameters at h=0. Around m=0, $\psi(m)=O(m^2)$ in the disordered phase (dotted magenta), $\psi(m)=O(m^4)$ along the critical line (dash-dotted blue line), while $\psi(m)=O(m^6)$ at the tricritical point (TCP) (solid red line). We also plot the large deviation function for J=0, K=1.25, h=0, $\beta=1$, which belongs to the ferromagnetic phase (green dashed line).

Large deviation function of the magnetization [Eq. (8)]

In Fig. 5, we plot the large deviation function $\psi(m)$ of the Nagle-Kardar model for different values of the parameters across the second order phase transition, see Eq. (8) in the main text. The probability distribution function of the magnetization M at finite N can be expressed in terms of $\psi(m)$ as $P_N(M) = \exp(-N\psi(m))$. The magenta dotted curve, obtained for J/T = 0 and K/T = 0.75, corresponds to the disordered phase: it has a unique minimum for $m = m^* = 0$, the equilibrium value of m, around which the function has a quadratic behavior. At the second-order transition line, $\psi(m) \sim m^4$ for small m (dash-dotted blue curve). At the tricritical point, $\psi(m) \sim m^6$ around m = 0 (full red line). Let us remark that in all these cases, the function $\psi(m)$ always vanishes at its minimum, meaning that, by increasing N, the probability distribution of m, $P_N(Nm)$, concentrates on its equilibrium value. The situation changes in the ferromagnetic phase (dashed green line), where the large deviation function valishes at two symmetric minima where $m^* \neq 0$.

Analytic expression of the transition probabilities of the master equation (10)

Let us comment on the computation of the transition rates $\mathcal{T}(M+\Delta M,2S+\Delta S|M,2S)$. As $\Delta M=\pm 2$ and $\Delta S=0,\pm 2$, there are in total six different types of transition rates to consider. Here, we sketch the computation of the transition rate $\mathcal{T}(M,2S|M+2,2S)$, corresponding to the transition from a configuration with total magnetization M+2 and 2S defects to one with magnetization M and still 2S defects. This transition occurs upon flipping a spin in the state +1 that is initially adjacent to a single defect, as for example $\dots + \oplus |--\dots \to \dots +| \bigcirc --\dots$, where the flipped spin is en-

circled. $\mathcal{T}(M,2S|M+2,2S)$ can be expressed as the product of two factors: $\mathcal{T}(M,2S|M+2,2S) = B_1^+(M+2,2S)A_{M+2\to M}^{2S\to 2S}$. The factor $B_1^+(M+2,2S)$ is the probability that a randomly selected spin in a configuration with magnetization M+2 and 2S defects is in the state +1 and adjacent to exactly one defect, and $A_{M+2\to M}^{2S\to 2S}$ is the probability of accepting the spin flip $M+2\to M$. The acceptance probability $A_{M+2\to M}^{2S\to 2S}$ takes the well-known Glauber form

$$A_{M+2\to M}^{2S\to 2S} = \frac{1}{1+e^{\Delta E/T}} = \frac{e^{-(K\frac{M+1}{N}+h)/T}}{2\cosh((K\frac{M+1}{N}+h)/T)}.$$
 (19)

Instead, the rate $B_1^+(M+2,2S)$ has a more cumbersome expression, as it depends on the specific spin configurations. Under some reasonable assumptions (see SM), it admits an explicit expression in terms of a sum of products of binomial coefficients, such that the rate only depends on the intensive variables m and s in the limit of large N.

A sketch of the derivation of the Fokker-Planck equation [Eq. (11)]

While the complete derivation of the Fokker-Planck equation is reported in the SM, here we sketch the basic ingredients. Let us thus consider the expansion in ϵ of the following term of the master equation (10):

$$\begin{split} \mathcal{T}(M,2S|M+2,2S)P_N(M+2,2S;t) + \\ -\mathcal{T}(M-2,2S|M,2S)P_N(M,2S;t) = \\ &= 2\epsilon \frac{\partial}{\partial m} \Big[\kappa_1^+(m,s) f_1^+(m) p(m,s;t) \Big] + \\ &+ 2\epsilon^2 \frac{\partial}{\partial m} \Big[f_1^+(m) \frac{\partial}{\partial m} \Big(\kappa_1^+(m,s) p(m,s;t) \Big) \Big] + O(\epsilon^3), \end{split}$$

where the functions $f_1^+(m)$ and $\kappa_1^+(m,s)$ are defined as

$$\kappa_1^+(m,s) = s \Big(1 - \frac{s}{1+m} \Big), \quad f_1^+(m) = \frac{e^{-(Km+h)/T}}{2\cosh\big((Km+h)/T\big)}.$$

The expression for $f_1^+(m)$ follows directly from Eq. (19). Instead, the probability $\kappa_1^+(m)$ for an up-spin to have exactly one down-spin neighbor, admits the following interpretation. The probability for a randomly selected spin to be in the state +1 in a configuration with magnetization m is $\frac{1+m}{2}$, since $\frac{N+M}{2}$ up-spins are present. On the other hand, the probability that a neighboring spin of an up-spin is in the state -1 is $\frac{s}{1+m}$. Indeed, there are 2S defects distributed among $\frac{N+M}{2}$ up-spins, so that the probability for an up-spin to have to its left (and similarly to its right) a down-spin is $\frac{1}{2}\frac{2S}{(N+M)/2} = \frac{s}{1+m}$. Consequently, the probability that a spin +1 is adjacent to exactly one down-spin neighbor is given by $\kappa_1^+(m,s) = 2\frac{s}{1+m}\left(1-\frac{s}{1+m}\right)$, where the factor 2 accounts for the two possible positions (left or right) of the neighboring spin -1.

Ginzburg criterion for the upper critical dimension

The Nagle-Kardar lattice model can be mapped in the thermodynamic limit onto a continuum field theory in terms of a scalar field ϕ . In units where the action is dimensionless, the scaling dimension of the field ϕ in space-dimension d is $\Delta_{\phi} = (d-2)/2$. On the second-order critical line, the Landau potential is of order ϕ^4 , while at the tricritical point it is of order ϕ^6 . In order to compute the upper critical dimension d_u , we use the Ginzburg criterion, by equating the dimension of the Landau potential to d. Therefore, at the critical point, we have to solve the algebraic equation 4(d-2)/2 = d, which has the unique solution $d = d_u = 4$. At the tricritical point, instead, the algebraic equation is 6(d-2)/2 = d that is solved by $d = d_u = 3$.

Center manifold theory: derivation of Eq. (17) in the main text

Along the second-order phase transition line $K/T = e^{-2J/T}$ of the Nagle-Kardar model, the fraction of defects is $s^* = K/(K+1)$ and the magnetization is $m^* = 0$. Close to this equilibrium, the dynamics of $\delta m \equiv x$ and $\delta s \equiv y$, up to terms of order 4 in $x^p y^q$, is given by

$$\frac{dx}{dt} = \dot{x} = (ay + by^2)x + (c + dy + ey^2)x^3,$$
 (20)

$$\frac{dy}{dt} = \dot{y} = Ay + By^2 + (C + Dy + Ey^2)x^2 + Fx^4, \quad (21)$$

where the coefficients $a, b, \dots, e, A, B, \dots, F$ depend only on the strength K of the mean-field coupling. In Eq. (20),

$$a = -\frac{2K(1+K)(K-1)^3}{(1+K^2)^2}, \quad b = -2K + \frac{8K^3}{(1+K^2)^2},$$

$$c = -\frac{2K^3(3+K-3K^2+K^3)}{3(1+K^2)^2},$$

while in Eq. (21),

$$A = -\frac{4K}{1+K^2}, \quad B = 2 - \frac{4}{1+K^2}, \quad C = -2 + \frac{2}{1+K^2},$$

$$D = -\frac{4\left[K + K^2(-1 + 2K - 3K^3 + K^4)\right]}{\left(1 + K^2\right)^3}.$$

We do not provide the expression of the coefficients e, E, F as they do not enter the derivations below.

The system of equations (20)-(21) can be rewritten as

$$\begin{pmatrix} \dot{x} \\ \dot{y} \end{pmatrix} = \begin{pmatrix} 0 & 0 \\ 0 & A \end{pmatrix} \begin{pmatrix} x \\ y \end{pmatrix} + \begin{pmatrix} (ay + by^2)x + (c + dy + ey^2)x^3 + fx^5 \\ By^2 + (C + Dy + Ey^2)x^2 + (F + Gy)x^4 \end{pmatrix}.$$
 (22)

The eigenvalues of the linearized system are $\lambda_1 = 0$ and $\lambda_2 = A < 0$. This means that the equilibrium point (0,0) is non-hyperbolic and we need to invoke the center manifold theory [55] to make further progress. The center manifold E^c of the

linearized system is the x-axis, as follows by computing the eigenvector corresponding to the eigenvalue $\lambda_1 = 0$. Hence, we parametrize the center manifold as

$$W^{c} = \{(x, y) : y = h(x), h(0) = 0, h'(0) = 0\}.$$
 (23)

The condition h(0) = 0 comes from the fact that the center manifold passes through the origin, while the condition h'(0) = 0 is due to the fact that W^c is tangential to E^c at the origin (0,0). To determine h(x), we express it in Taylor expansion by setting $y = h(x) = \alpha x^2 + \gamma x^3 + \delta x^4 + \zeta x^5 + O(x^6)$. On the one hand, from Eq. (21), we get

$$\dot{y} = (A\alpha + C)x^2 + A\gamma x^3 + (F + D\alpha + B\alpha^2 + A\delta)x^4 + (D\gamma + 2B\alpha\gamma + A\zeta)x^5 + O(x^6). \tag{24}$$

On the other hand, from Eq. (20), we obtain

$$\dot{y} = h'(x)\dot{x} = (2c\alpha + 2a\alpha^2)x^4 + (3c\gamma + 5a\alpha\gamma)x^5.$$
 (25)

Therefore, equating Eqs. (24)-(25), we deduce that

$$A\gamma = 0 \Rightarrow \gamma = 0 \ (A \neq 0),$$

 $A\alpha + C = 0 \Rightarrow \alpha = -C/A,$
 $F + D\alpha + B\alpha^2 + A\delta = 2c\alpha + 2a\alpha^2,$
 $D\gamma + 2B\alpha\gamma + A\zeta = 3c\gamma + 5a\alpha\gamma.$

At order 3 in x,

$$y = h(x) = -\frac{C}{A}x^2 + O(x^4) = -\frac{K}{2}x^2 + O(x^4).$$
 (26)

Hence, it follows that

$$\dot{x} = \left(c - a\frac{C}{A}\right)x^3 + O(x^5) = \frac{K^2(K^2 - 3)}{3(1 + K^2)}x^3 + O(x^5), \quad (27)$$

which is Eq. (17) of the main text.

SUPPLEMENTAL MATERIAL

In the sections below, we report all the derivations for the results reported in the main text. In this Supplemental Material the symbol β denotes the inverse temperature, namely $\beta = 1/T$ with k_B set to 1, differently to the main text where β is one of the static critical exponents that define the decay of the average absolute magnetization $\langle |m(t, N)| \rangle$.

NAGLE-KARDAR MODEL: FREE ENERGY AND PHASE DIAGRAM IN THE CANONICAL ENSEMBLE

Let us consider the Hamiltonian

$$H = -J\sum_{i=1}^{N} s_i s_{i+1} - \frac{K}{2N} \left(\sum_{i=1}^{N} s_i\right)^2 - h\sum_{i=1}^{N} s_i,$$
(28)

where N is the number of spins, $s_i \in \{-1, +1\}$, and the parameters J, K and h represent the nearest-neighbor coupling strength, the mean-field coupling strength and the external field, respectively. Throughout, periodic boundary conditions are assumed, i.e., $s_{N+1} = s_1$. The equilibrium probability to observe a spin configuration $C = (s_1, \dots, s_N)$ is given by the Gibbs measure

$$\omega_N(C) = \frac{e^{-\beta H(C)}}{Z_N},\tag{29}$$

where $Z_N = \sum_C \omega_N(C)$ denotes the partition function. The latter can be evaluated in the thermodynamic limit $N \to \infty$ using the Hubbard-Stratonovich transformation. Specifically, using the identity

$$e^{\frac{\beta K}{2N} \left(\sum_{i=1}^{N} s_i\right)^2} = \sqrt{\frac{N\beta K}{2\pi}} \int_{-\infty}^{+\infty} dx \, e^{-\frac{N\beta K}{2} x^2} e^{\beta K x \sum_{i=1}^{N} s_i},\tag{30}$$

the partition function reads as

$$Z_{N} = \sum_{C} \sqrt{\frac{N\beta K}{2\pi}} \int_{-\infty}^{+\infty} dx \, e^{\beta J \sum_{i=1}^{N} s_{i} s_{i+1}} e^{-\frac{N\beta K}{2} x^{2}} e^{\beta (Kx+h) \sum_{i=1}^{N} s_{i}} =$$

$$= \sqrt{\frac{N\beta K}{2\pi}} \int_{-\infty}^{+\infty} dx \, e^{-\frac{N\beta K}{2} x^{2}} \operatorname{Tr}(V^{N}),$$
(31)

where the 2×2 transfer matrix V is given by

$$V = \begin{pmatrix} e^{\beta J + \beta(Kx+h)} & e^{-\beta J} \\ e^{-\beta J} & e^{\beta J - \beta(Kx+h)} \end{pmatrix}. \tag{32}$$

The eigenvalues $\lambda_{\pm}(x)$ of the transfer matrix V are

$$\lambda_{\pm}(x) = e^{\beta J} \cosh\left(\beta(Kx+h)\right) \pm \sqrt{e^{2\beta J} \sinh^2\left(\beta(Kx+h)\right) + e^{-2\beta J}}.$$
 (33)

In the large N limit, the eigenvalue $\lambda_+(x)$ is dominant, with the result that

$$Z_N \sim \sqrt{\frac{N\beta K}{2\pi}} e^{-\beta N \left[\frac{K}{2}x^{*2} - \frac{1}{\beta}\log(\lambda_+(x^*))\right]},\tag{34}$$

where x^* is the absolute minimum of the free-energy density $\mathcal{F}(\beta, J, K, h; x)$ given by

$$\mathcal{F}(\beta, J, K, h; x) = \frac{K}{2}x^2 - \frac{1}{\beta}\log(\lambda_+(x)). \tag{35}$$

Explicit computations show that x^* is solution of the implicit equation

$$x^* = \frac{\sinh(\beta(h + Kx^*))}{\sqrt{\sinh^2(\beta(h + Kx^*)) + e^{-4\beta J}}}.$$
 (36)

The free energy $f(\beta, J, K, h)$ per site is then given by

$$f(\beta, J, K, h) = \mathcal{F}(\beta, J, K, h; x^*). \tag{37}$$

The absolute minimum x^* coincides with the magnetization per site

$$m^* := \lim_{N \to +\infty} \frac{1}{N} \sum_{i=1}^{N} \langle s_i \rangle. \tag{38}$$

Indeed, we have:

$$m^* = -\frac{\partial}{\partial h} f(\beta, J, K, h) = -\frac{\partial}{\partial h} \mathcal{F}(\beta, J, K, h; x^*) = \frac{1}{\beta K} \frac{\partial}{\partial x} \log (\lambda_+(x))|_{x=x^*} = x^*.$$
 (39)

The magnetization m^* is thus the global minimum of the free-energy density $\mathcal{F}(\beta, J, K, h; m)$ whose expression is

$$\mathcal{F}(\beta, J, K, h; m) = \frac{K}{2}m^2 - \frac{1}{\beta}\log(\lambda_+(m))$$
(40)

$$= \frac{K}{2}m^2 - J - \frac{1}{\beta}\log\left[\cosh(\beta(Km+h)) + \sqrt{\sinh^2(\beta(Km+h)) + e^{-4\beta J}}\right]. \tag{41}$$

Formally, Eq. (36) may admit several solutions. Among them, only the one that minimizes $\mathcal{F}(\beta, J, K, h; m)$ corresponds to the equilibrium magnetization in the thermodynamic limit. In the absence of the external field (i.e., for h = 0), $\mathcal{F}(\beta, J, K, h = 0; m)$ is symmetric in m and its Taylor expansion around m = 0 reads as

$$\mathcal{F}(\beta, J, K, h = 0; m) = -\frac{1}{\beta} \log(2 \cosh(\beta J)) + \frac{1}{2} K \left(1 - \frac{\beta K}{e^{-2\beta J}}\right) m^2 + \frac{\beta^3 K^4 (-1 + 3e^{4\beta J})}{24e^{-2\beta J}} m^4 + O(m^6). \tag{42}$$

A second-order phase transition occurs when the coefficient of the quadratic term vanishes, i.e., when $\beta K = e^{-2\beta J}$; see solid red line in Fig. 6 (Left). This second-order line ends at a *tricritical point* (red square in the figure), where both the quadratic and quartic coefficients of $\mathcal{F}(\beta, J, K, h; m)$ in m simultaneously vanish. This condition corresponds to set

$$(\beta J, \beta K) = \left(-\frac{\log(3)}{4}, \sqrt{3}\right). \tag{43}$$

For values $\beta J < -\frac{\log(3)}{4}$ and $\beta K > \sqrt{3}$, the system exhibits a line of first-order phase transitions that is characterized by a discontinuous jump in the magnetization, as depicted by the dashed red line in Fig. 6 (Left). The different behaviours of m^* as a function of βK are illustrated in Fig. 6 (Right).

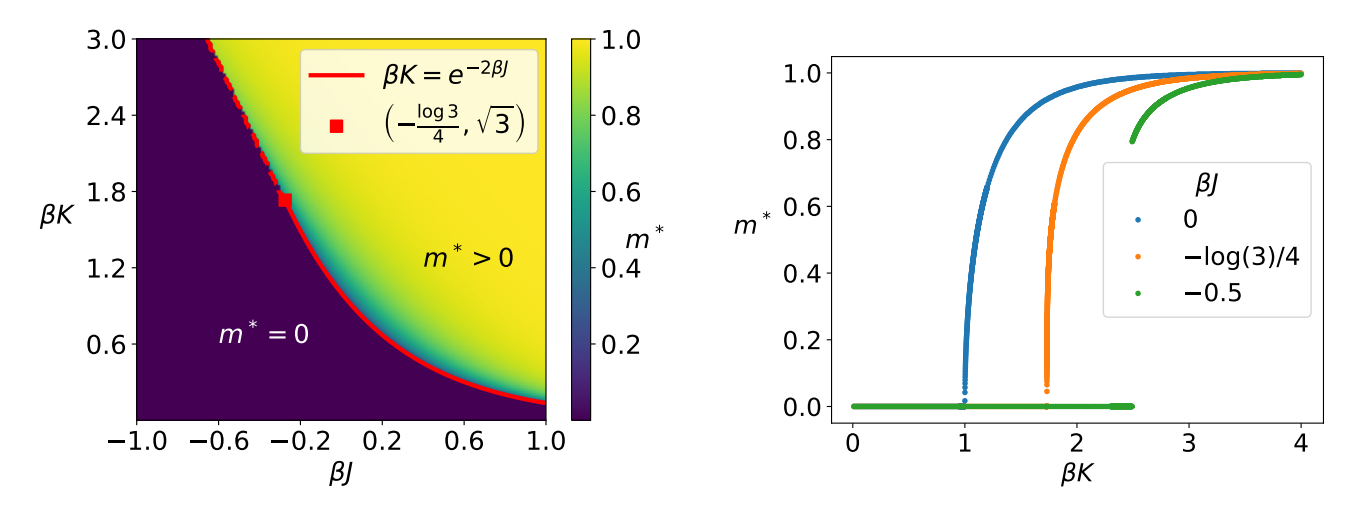


FIG. 6: (Left) Phase diagram of the magnetization m^* in the canonical ensemble for h=0. A tricritical point (red square) marks the junction between a continuous (second-order) transition line (solid red) and a discontinuous (first-order) one (dashed red). (Right) Equilibrium magnetization m^* as a function of βK for $\beta J=0$ (second-order transition), $\beta J=-\log(3)/4$ (tricritical point) and $\beta J=-0.5$ (first-order transition).

JOINT PROBABILITY DISTRIBUTION OF THE TOTAL MAGNETIZATION AND THE NUMBER OF DEFECTS

The Hamiltonian Eq. (28) can be equivalently expressed in terms of both the total magnetization $M = \sum_{i=1}^{N} s_i$ and the number of defects. A defect is a formal representation of the presence of a pair of adjacent spins with opposite signs. Under periodic boundary conditions, the number of defects is always even and given by $2S = \sum_{i=1}^{N} (1 - s_i s_{i+1})/2$. In terms of M and S, the Hamiltonian Eq. (28) becomes

$$H = -J(N - 4S) - \frac{K}{2N}M^2 - hM. \tag{44}$$

Note that the total magnetization M ranges from -N to +N in steps of 2, while the number of defects 2S takes values from $2(1-\delta_{|M|,N})$ to N-|M| also in steps of 2 (δ_{ij} is the Kronecker delta). Indeed, given a configuration with magnetization $0 \le M < N$, the minimum number of defects is 2 that occurs when all down-spins are contiguous. On the other hand, the number of defects is maximized when each down-spin is isolated, i.e., surrounded by up-spins on both sides, which leads to N-M defects (since there are (N-M)/2 down-spins). A similar argument holds for negative magnetization -N < M < 0. In the fully polarized cases $M = \pm N$, 2S = 0 as no defects are present.

The goal of this section is to derive an exact expression for the equilibrium joint probability distribution $P_N(M, 2S)$ of configurations of N spins with total magnetization M and 2S defects. Then, we will analyze the large-deviation behavior of $P_N(M, 2S)$.

Exact expressions for finite-size systems

The statistical weight $\omega_N(M, 2S)$ of any configuration with total magnetization M and 2S defects at equilibrium is

$$\omega_N(M, 2S) = \frac{e^{\beta J(N-4S) + \frac{\beta K}{2N}M^2 + \beta hM}}{Z_N},\tag{45}$$

where the partition function $Z_N = \sum_{M,S} \omega_N(M,2S)$ is given by the weighted sum of configurations. The exponent N-4S comes from the fact that there are N-2S nearest-neighbor spin pairs with the same orientation and 2S pairs with opposite orientation. Consequently, the joint probability $P_N(M,2S)$ of observing a configuration with magnetization M and 2S defects reads:

$$P_N(M, 2S) = \Omega_N(M, 2S)\omega_N(M, 2S) = \Omega_N(M, 2S) \frac{e^{\beta J(N-4S) + \frac{\beta K}{2N}M^2 + \beta hM}}{Z_N},$$
(46)

where $\Omega_N(M, 2S)$ enumerates the distinct configurations with magnetization M and 2S defects. The expression of $\Omega_N(M, 2S)$ can be computed explicitly [61], and it is given by

$$\Omega_N(M, 2S) = \binom{\frac{N+M}{2} - 1}{S - 1} \binom{\frac{N-M}{2}}{S} + \binom{\frac{N-M}{2} - 1}{S - 1} \binom{\frac{N+M}{2}}{S} + \delta_{M, \pm N} \delta_{S, 0}, \tag{47}$$

where the binomial coefficients are understood to be zero whenever any of their arguments are negative or non-integer.

The first two terms are obtained as follows. First, recall that in a configuration of N spins with magnetization M, there are $\frac{N+M}{2}$ up-spins and $\frac{N-M}{2}$ down-spins. In the presence of 2S defects, exactly S of them lie to the right (left) of a down-spin, while the other lie to the right (left) of an up-spin. Suppose the first spin is a spin -1, as in the following example:

There are $\left(\frac{N-M}{S}\right)$ distinct ways of placing S defects among the $\frac{N-M}{2}$ down-spins, partitioning the down-spins into S consecutive groups of sizes v_1, v_2, \ldots, v_S , each of them containing at least one spin. In the example, N=11 (plus a spin, encircled, determined by the boundary condition), M=-3, $v_1=2$, $v_2=3$, $v_3=2$. Similarly, one has to distribute the S defects among the $\frac{N+M}{2}$ up-spins, with the constraint that the last up-spin is immediately followed by a defect. This can be done in $\left(\frac{N+M}{S-1}\right)$ distinct ways. In the example, $\mu_1=2$, $\mu_2=1$ and $\mu_3=1$. The resulting configuration is formed by alternating the groups of sizes v_i and u_i for $i=1,\ldots,S$. The total number of such configurations corresponds to the first term of Eq. (47). The second term in Eq. (47) is derived similarly, with the assumption that the first spin is an up-spin.

The last term of $\Omega_N(M, 2S)$ accounts for two specific configurations in which all spins are either up (+1) or down (-1); in these cases, the product of Kronecker deltas is equal to 1 with the result that $\Omega_N(M = \pm N, 2S = 0) = 1$. Hence, the exact expression of the joint probability $P_N(M, 2S)$ is

$$P_N(M, 2S) = \left[\binom{\frac{N+M}{2} - 1}{S - 1} \binom{\frac{N-M}{2}}{S} + \binom{\frac{N-M}{2} - 1}{S - 1} \binom{\frac{N+M}{2}}{S} + \delta_{M, \pm N} \delta_{S, 0} \right] \frac{e^{\beta J(N - 4S) + \frac{\beta K}{2N} M^2 + \beta hM}}{Z_N}. \tag{48}$$

The marginal probability distributions for the magnetization and the number of defects can be obtained by summing the joint distribution over the appropriate variable

$$P_N(M) = \sum_{S=0}^{\lfloor N/2 \rfloor} P_N(M, 2S) \quad \text{and} \quad P_N(2S) = \sum_{M=-N}^{N} P_N(M, 2S), \tag{49}$$

where $\lfloor x \rfloor$ denotes the largest integer smaller or equal to x. In this regard, it is worth noting that the probability $P_N(M)$ can be expressed in terms of hypergeometric functions. This can be seen by computing the summation

$$\sum_{S=1}^{\lfloor N/2 \rfloor} {\binom{N+M}{2} - 1 \choose S - 1} {\binom{N-M}{2} \choose S} \frac{e^{\beta J(N-4S) + \frac{\beta K}{2N} M^2 + \beta hM}}{Z_N} = \frac{e^{\beta JN + \frac{\beta K}{2N} M^2 + \beta hM}}{Z_N} \sum_{S=1}^{\lfloor N/2 \rfloor} {\binom{N+M}{2} - 1 \choose S - 1} {\binom{N-M}{2} \choose S} x^S, \tag{50}$$

with $x = e^{-4\beta J}$. Let us first assume N to be even. In that case, we have

$$\sum_{S=1}^{N/2} {N+M \choose S-1} {N-M \choose S} x^S = x \sum_{S=0}^{N/2-1} {N+M \choose S} (1) \left(\frac{N-M}{2} \right) x^S =$$

$$= x \sum_{S=0}^{N/2-1} \frac{(\frac{N+M}{2} - 1)!}{S!(\frac{N+M}{2} - S - 1)!} \frac{(\frac{N-M}{2})!}{(S+1)!(\frac{N-M}{2} - S - 1)!} x^S =$$

$$= x \frac{N-M}{2} \sum_{S=0}^{N/2-1} \frac{(\frac{N+M}{2} - 1)!}{S!} \frac{(\frac{N-M}{2} - 1)!}{(S+1)!(\frac{N-M}{2} - S - 1)!} x^S ,$$

$$(51)$$

where

$$(\alpha)_{\underline{S}} := \alpha(\alpha - 1) \cdots (\alpha - S + 1) = \frac{\alpha!}{(\alpha - S)!},$$

$$(\alpha)_{\overline{S}} := \alpha(\alpha + 1) \cdots (\alpha + S - 1) = \frac{(\alpha + S - 1)!}{(\alpha - 1)!},$$
(52)

are respectively the falling and the rising factorials [62], each given by the product of S terms. The rising and falling factorials are related by the following identity:

$$(\alpha)_S = (-1)^S (-\alpha)_{\overline{S}}. \tag{53}$$

Using this identity, it holds that

$$\sum_{S=1}^{N/2} {N+M \choose 2} - 1 \choose {S-1} \binom{N-M}{2} S x^S = x \frac{N-M}{2} \sum_{S=0}^{N/2-1} \frac{(1 - \frac{N+M}{2})_{\overline{S}} (1 - \frac{N-M}{2})_{\overline{S}}}{(2)_{\overline{S}}} \frac{x^S}{S!}.$$
 (54)

One can extend the summation to infinity without modifying the result, which leads to

$$\sum_{S=1}^{N/2} {N+M \choose S-1} {N-M \choose S} x^{S} = x \frac{N-M}{2} \sum_{S=0}^{\infty} \frac{(1-\frac{N+M}{2})_{\overline{S}}(1-\frac{N-M}{2})_{\overline{S}}}{(2)_{\overline{S}}} \frac{x^{S}}{S!} =$$

$$= x \frac{N-M}{2} {}_{2}F_{1} \left(1-\frac{N+M}{2}, 1-\frac{N-M}{2}; 2; x\right),$$
(55)

where ${}_{2}F_{1}(a,b,c;z)$ denotes the hypergeometric function defined by the series [63]

$${}_{2}F_{1}(a,b;c;z) := \sum_{n=0}^{\infty} \frac{(a)_{\overline{n}}(b)_{\overline{n}}}{(c)_{\overline{n}}} \frac{z^{n}}{n!}.$$
 (56)

The same expression is obtained when N is odd. We now turn our attention to the second sum given by

$$\frac{e^{\beta JN + \frac{\beta K}{2N}M^2 + \beta hM}}{Z} \sum_{S=1}^{\lfloor N/2 \rfloor} {\frac{N-M}{2} - 1 \choose S - 1} {\frac{N+M}{2} \choose S} x^S.$$
 (57)

Following the same reasoning as above, we get that

$$\sum_{S=1}^{\lfloor N/2 \rfloor} {N-M \choose S-1} {N+M \choose S} x^S = x \sum_{S=0}^{\lfloor N/2 \rfloor - 1} {N-M \choose S} {1 \choose S-1} x^S =$$

$$= x \frac{N+M}{2} \sum_{S=0}^{\lfloor N/2 \rfloor - 1} \frac{{N-M \choose 2}-1}{2 \choose S-1} \frac{{N+M \choose 2}}{(2)_S} x^S =$$

$$= x \frac{N+M}{2} {2F_1} \left(1 - \frac{N+M}{2}, 1 - \frac{N-M}{2}; 2; x\right).$$

$$(58)$$

Combining all the computed terms, we finally obtain

$$P_N(M) = N \frac{e^{\beta J(N-4) + \frac{\beta K}{2N}M^2 + \beta hM}}{Z_N} \cdot {}_2F_1\left(1 - \frac{N+M}{2}, 1 - \frac{N-M}{2}, 2; e^{-4\beta J}\right). \tag{59}$$

Large-deviation behaviors and static (tri)critical exponents

The purpose of this section is to provide an asymptotic expression for the probability $P_N(M)$ in the limit of large N. This is done by using the asymptotic expression of the hypergeometric functions derived in [64]. In particular, we will use the following asymptotic formula, valid for a, b, c real

$$_{2}F_{1}(a-\varepsilon\lambda,\ b-\lambda;c;z) \sim \frac{\Gamma(c)(\varepsilon\lambda)^{\frac{1}{2}-c}}{\sqrt{2\pi|\varepsilon-1|\sigma(z)}} \cdot \frac{(1-\xi)^{c-a+\varepsilon\lambda}}{(-\xi)^{\varepsilon\lambda-a}(1-z\xi)^{b-\lambda}} \quad \text{as} \quad \lambda \to \infty,$$
 (60)

where

$$\xi = \frac{1 - \epsilon}{2} - \frac{|1 - \epsilon|}{2} \sigma(z) \quad \text{with} \quad \sigma(z) = \sqrt{1 + \frac{4\epsilon}{(\epsilon - 1)^2 z}}.$$
 (61)

In our case,

$$\lambda \equiv \lambda(m) = \frac{N - M}{2} = N \frac{1 - m}{2}, \quad \epsilon \equiv \epsilon(m) = \frac{N + M}{N - M} = \frac{1 + m}{1 - m}, \quad a = 1, \quad b = 1, \quad c = 2, \quad z = e^{-4\beta J}.$$
 (62)

Thus, inserting the latter parameters into Eq. (59) leads, after a few simplifications, to

$$P_{N}(M) \approx e^{-N\psi(m)},$$

$$\psi(m) = -\beta J - \beta h m - \frac{\beta K}{2} m^{2} - \beta f - \frac{1+m}{2} \log\left(1 - \frac{1}{\xi(m)}\right) - \frac{1-m}{2} \log\left(1 - e^{-4\beta J} \xi(m)\right),$$
(63)

with $f \equiv \mathcal{F}(\beta, J, K, h; m^*)$ the free-energy of the system, introduced previously.

In the disordered phase and for h = 0, the function $\psi(m)$ admits the following expansion around m = 0:

$$\psi(m) = \frac{e^{-2\beta J} - \beta K}{2} m^2 + \frac{3e^{4\beta J} - 1}{24e^{6\beta J}} m^4 + \frac{15 - 10e^{-4\beta J} + 3e^{-8\beta J}}{240e^{2\beta J}} m^6 + O(m^8). \tag{64}$$

In the disordered phase and away from the second-order transition line $\beta K = e^{-2\beta J}$, the large deviation function is quadratic around m=0. In contrast, on the line $\beta K=e^{-2\beta J}$, $\psi(m)$ has a quartic behavior around m=0, except at the tricritical point where the coefficient in m^4 also vanishes. From this analysis, we also deduce that $|m^*| \sim N^{-1/2}$ in the disordered phase and away from the second-order transition line, while $|m^*| \sim N^{-1/4}$ along the second-order line $\beta K=e^{-2\beta J}$, except at the tricritical point where $|m^*| \sim N^{-1/6}$.

In the large *N* limit, the use of the Stirling formula $n! \sim \sqrt{2\pi n}(n/e)^n$ allows us to extract the dominant behavior of also $P_N(M, 2S)$, which is provided by the following expression in large-deviation form [45]:

$$P_N(M, 2S) \sim e^{-NU(m,s)},$$
 (65)

where

$$U(m,s) = s \log(s) - \frac{1+m}{2} \log(1+m) - \frac{1-m}{2} \log(1-m) + \frac{1+m-s}{2} \log(1+m-s) + \frac{1-m-s}{2} \log(1-m-s) + -\beta \left(\frac{K}{2}m^2 + hm + J(1-2s) + f\right).$$
(66)

GLAUBER DYNAMICS AND MASTER EQUATION

In this section we provide the formal derivation of the master equation governing the time evolution of the joint probability $P_N(M, 2S; t)$ under Glauber dynamics. Let us recall that the number 2S of defects separating two spins with opposite sign is always even. The Glauber dynamics proceeds as follows: starting from an initial configuration, a single spin is randomly selected at each discrete time step, and a flip is attempted. Denoting with ΔE the energy change associated with this flip, the move is accepted with probability $\frac{1}{1+e^{\beta\Delta E}}$. Note that, upon acceptance of a single flip, the total number of up-spins increases or decreases by 2, while the number of defects either remains unchanged or changes by ± 2 . Let $C = (s_1, \dots, s_N)$ denote one of the 2^N distinct spin configurations. Then the probability of observing a configuration C evolves in time according to the following master equation:

$$\frac{\partial P(C,t)}{\partial t} = -\sum_{i}^{N} \mathcal{T}_{M\to M-2s_{i}}^{2S\to 2S}(s_{i}\to -s_{i}|C)P(C,t) - \sum_{i}^{N} \mathcal{T}_{M\to M-2s_{i}}^{2S\to 2S+2}(s_{i}\to -s_{i}|C)P(C,t) + \\
-\sum_{i}^{N} \mathcal{T}_{M\to M-2s_{i}}^{2S\to 2S-2}(s_{i}\to -s_{i}|C)P(C,t) + \sum_{i}^{N} \mathcal{T}_{M+2s_{i}\to M}^{2S\to 2S}(s_{i}\to -s_{i}|C')P(C',t) + \\
+\sum_{i}^{N} \mathcal{T}_{M+2s_{i}\to M}^{2S+2\to 2S}(s_{i}\to -s_{i}|C')P(C',t) + \sum_{i}^{N} \mathcal{T}_{M+2s_{i}\to M}^{2S-2\to 2S}(s_{i}\to -s_{i}|C')P(C',t). \tag{67}$$

The transition rates \mathcal{T} can be decomposed as

$$\mathcal{T}_{M \to M'}^{2S \to 2S'}(s_i \to -s_i|C) = I_{M \to M'}^{2S \to 2S'}(s_i \to -s_i|C) A_{M \to M'}^{2S \to 2S'}, \tag{68}$$

where

- $A_{M \to M'}^{2S \to 2S'}$ denotes the acceptance probability of a spin flip, which changes the magnetization from M to M' and the number of defects from 2S to 2S'. This probability depends solely on the associated energy change, not on the specific configuration.
- $I_{M \to M'}^{2S \to 2S'}(s_i \to -s_i|C)$ is an indicator function that takes the value 1 if flipping site *i* in configuration *C* changes the magnetization from *M* to *M'* and the number of defects from 2*S* to 2*S'*.

As anticipated previously, we are interested in the probability

$$P_N(M, 2S; t) = \sum_{C} \delta(\sum_{i} s_i, M) \delta(\sum_{i} \frac{1 - s_i s_{i+1}}{2}, 2S) P(C, t),$$
(69)

where the sum runs over all the 2^N distinct spin configurations C. Using Eq. (67), the time evolution of $P_N(M, 2S; t)$ is given by:

$$\frac{\partial P_{N}(M, 2S; t)}{\partial t} = -\sum_{C} \delta \left(\sum_{i} s_{i}, M \right) \delta \left(\sum_{i} \frac{1 - s_{i} s_{i+1}}{2}, 2s \right) \sum_{i=1}^{N} \mathcal{T}_{M \to M-2}^{2S \to 2S}(s_{i} = +1 \to s_{i} = -1 | C) P(C, t) + \\
- \sum_{C} \delta \left(\sum_{i} s_{i}, M \right) \delta \left(\sum_{i} \frac{1 - s_{i} s_{i+1}}{2}, 2s \right) \sum_{i=1}^{N} \mathcal{T}_{M \to M+2}^{2S \to 2S}(s_{i} = -1 \to s_{i} = +1 | C) P(C, t) + \\
+ \left(\text{the other terms entering Eq. (67)} \right).$$
(70)

In particular, let us consider the first term in Eq. (70); the discussion is then similar for the other terms. As mentioned before, the transition rate $\mathcal{T}_{M \to M-2}^{2S \to 2S}(s_i = +1 \to s_i = -1|C)$ can be decomposed as a product of two terms namely:

$$\mathcal{T}_{M \to M-2}^{2S \to 2S}(s_i = +1 \to s_i = -1 | C) = I_{M \to M-2}^{2S \to 2S}(s_i = +1 \to s_i = -1 | C) A_{M \to M-2}^{2S \to 2S}. \tag{71}$$

To obtain a closed expression for the time evolution of $P_N(M, 2S; t)$, one has to get rid off the explicit (a priori) dependence of the indicator function $I_{M\to M-2}^{2S\to 2S}(s_i=+1\to s_i=-1|C)$ on the microscopic configurations C. This indicator function evaluates to 1 if spin s_i , in configuration C with magnetization M and 2S defects, is equal to +1 and adjacent to a single defect. Thus, for the first term in Eq. (70), we have

$$\sum_{C} \delta\left(\sum_{i} s_{i}, M\right) \delta\left(\sum_{i} \frac{1 - s_{i} s_{i+1}}{2}, 2S\right) \sum_{i=1}^{N} \mathcal{T}_{M \to M-2}^{2S \to 2S}(s_{i} = +1 \to s_{i} = -1 | C) P(C, t) = A_{M \to M-2}^{2S \to 2S} \sum_{k \ge 0} k \widetilde{P}_{N}(M, 2S, k; t), \tag{72}$$

where $\widetilde{P}_N(M, 2S, k; t)$ denotes the probability to observe a configuration with magnetization M, 2S defects and k up-spins surrounded by a single defect at time t. Then, we use the definition of conditional probability

$$\widetilde{P}_{N}(M, 2S, k; t) = P_{N}(k|M, 2S; t)P_{N}(M, 2S; t) =$$

$$\approx \frac{\Omega_{1}^{+}(N, M, 2S, k)}{\Omega_{N}(M, 2S)}P_{N}(M, 2S; t),$$
(74)

where, to get from the first to the second line, we used the assumption that the system explores all microstates with equal probability, once given the values of N, M and 2S at time t. This allows us to replace the time-dependent conditional probability $P_N(k|M, 2S; t)$ with a time-independent combinatorial factor. Specifically, $\Omega_1^+(N, M, 2S, k)$ denotes the number of *all* possible configurations with magnetization M, 2S defects and k up-spins (superscript +) surrounded by a single defect (subscript 1), while $\Omega_N(M, 2S)$ was defined in Eq. (47).

Proceeding similarly for the other terms, we can obtain a closed expression for $\frac{\partial}{\partial t}P_N(M,2S;t)$, i.e.,

$$\frac{\partial P_{N}(M,2S;t)}{\partial t} = -\left[A_{M\to M-2}^{2S\to 2S}B_{1}^{+}(N,M,2S) + A_{M\to M+2}^{2S\to 2S}B_{1}^{-}(N,M,2S)\right]P_{N}(M,2S;t) + \\ -\left[A_{M\to M-2}^{2S\to 2S+2}B_{0}^{+}(N,M,2S) + A_{M\to M+2}^{2S\to 2S+2}B_{0}^{-}(N,M,2S)\right]P_{N}(M,2S;t) + \\ -\left[A_{M\to M-2}^{2S\to 2S-2}B_{2}^{+}(N,M,2S) + A_{M\to M+2}^{2S\to 2S-2}B_{2}^{-}(N,M,2S)\right]P_{N}(M,2S;t) + \\ +A_{M+2\to M}^{2S\to 2S}B_{1}^{+}(N,M+2,2S)P_{N}(M+2,2S;t) + A_{M\to M+2}^{2S\to 2S}B_{1}^{-}(N,M-2,2S)P_{N}(M-2,2S;t) + \\ +A_{M+2\to M}^{2S+2\to 2S}B_{2}^{+}(N,M+2,2S+2)P_{N}(M+2,2S+2;t) + A_{M-2\to M}^{2S+2\to 2S}B_{2}^{-}(N,M-2,2S+2)P_{N}(M-2,2S+2;t) + \\ +A_{M+2\to M}^{2S-2\to 2S}B_{0}^{+}(N,M+2,2S-2)P_{N}(M+2,2S-2;t) + A_{M-2\to M}^{2S-2\to 2S}B_{0}^{-}(N,M-2,2S-2)P_{N}(M-2,2S-2;t),$$
 (75)

with

$$B_i^{\pm}(N, M, 2S) := \left(\sum_{k \ge 0} k \frac{\Omega_i^{\pm}(N, M, 2S, k)}{\Omega_N(M, 2S)} \right). \tag{76}$$

In the following subsections, we will determine the explicit expressions of both the acceptance probabilities A, and the combinatorial factors $B_i^{\pm}(N, M, 2S)$.

Acceptance probabilities

Let $\Delta E = E_{\text{new}} - E_{\text{old}}$ denote the energy change resulting from a transition between a configuration of energy E_{old} to one with energy E_{new} . Thus, the acceptance probability under the Glauber dynamics is given by $(1 + e^{\beta \Delta E})^{-1}$. We distinguish three cases depending on how the number of defects is affected by the single flip.

• First we consider the case in which flipping the spin *i* leaves unchanged the number of defects, i.e., $M \to M - 2s_i$ and $2S \to 2S$. In such case, the energy of the new and old configurations are respectively given by

$$E_{\text{new}} = -J(N - 4S) - \frac{K}{2N}(M - 2s_i)^2 - h(M - 2s_i),$$

$$E_{\text{old}} = -J(N - 4S) - \frac{K}{2N}M^2 - hM.$$
(77)

Hence, the resulting acceptance probability reads as

$$A_{M \to M-2s_i}^{2S \to 2S} = \frac{e^{-\beta s_i [K(M-s_i)/N+h]}}{2\cosh\{\beta [K(M-s_i)/N+h]\}}.$$
(78)

• Next we consider the case in which flipping the spin *i* reduces the number of defects by 2, i.e., $M \to M - 2s_i$ and $2S \to 2S - 2$. The energy of the configurations after and before the flip are

$$E_{\text{new}} = -J(N - 2(2S - 2)) - \frac{K}{2N}(M - 2s_i)^2 - h(M - s_i),$$

$$E_{\text{old}} = -J(N - 4S) - \frac{K}{2N}M^2 - hM,$$
(79)

and the acceptanceprobability is

$$A_{M \to M^{-2}S_i}^{2S \to 2S - 2} = \frac{e^{-\beta s_i [K(M - s_i)/N + h - 2Js_i]}}{2\cosh\{\beta [K(M - s_i)/N + h - 2Js_i]\}}.$$
(80)

• Finally, we consider the case where flipping the spin *i* increases the number of defects by 2, i.e., $M \rightarrow M - 2s_i$ and $2S \rightarrow 2S + 2$. The acceptance probability for this local move is the following:

$$A_{M \to M-2s_i}^{2S \to 2S+2} = \frac{e^{-\beta s_i [K(M-s_i)/N + h + 2Js_i]}}{2\cosh\{\beta [K(M-s_i)/N + h + 2Js_i]\}}.$$
(81)

Combinatorial enumerations

We now turn our attention to the computation of the coefficients $\Omega_i^{\pm}(N, M, 2S, k)$ that enumerate configurations of N spins with magnetization M, 2S defects and k spins ± 1 surrounded by i defects (i = 0, 1, 2). We start with the enumeration of up-spins surrounded by a single defect.

Enumeration of up-spins adjacent to a single barrier

Let us first note that the number of up-spins adjacent to a single defect must be even. To see this, first remove all +1 spins that are surrounded by two defects. This leaves an even number of defects, each paired with exactly one remaining +1 spin. Since no two defects share the same +1 spin (these defects have been removed), the total number of such spins must be even.

Proposition 1. The number $\Omega_1^+(N, M, 2S, 2k)$ of configurations of N spins, magnetization M, 2S defects and 2k up-spins (+1) adjacent to a single barrier is:

$$\Omega_{1}^{+}(N,M,2S,2k) = \begin{cases} \frac{2N}{N-M} {N-M \choose \frac{N-M}{2}} & if S = \frac{N+M}{2} \ and \ k = 0, \\ \frac{2N}{N-M} {N-M \choose 2} & otherwise. \end{cases}$$
(82)

The expression of $\Omega_1^+(N, M, 2S, 2k)$ given by Eq. (82) is valid for any parity of N and M. However, M and N must share the same parity (M = -N, -N + 2, ..., N - 2, N); otherwise, some binomial coefficients would involve half-integers, yielding zero. Moreover, Eq. (82) holds if M < N and $k \ge 1$. When M = N, all spins are +1 and there is no defect. We thus have $\Omega_1^+(N, N, 0, 0) = 1$. The number $\Omega_1^+(N, M, 2S, 2k)$ grows exponentially with the extensive variables; its growth rate given by the following proposition.

Proposition 2. Let us introduce the intensive (rescaled by N) variables:

$$m := \frac{M}{N}, \quad \kappa := \frac{2k}{N}, \quad s := \frac{2S}{N}. \tag{83}$$

Then, we have

$$\lim_{N \to +\infty} \frac{\log\left(\Omega_1^+(N, M, 2S, 2k)\right)}{N} = \frac{1}{2} f_1(m, s, \kappa),\tag{84}$$

with

$$f_1(m, s, \kappa) = -(s - \kappa)\log(s - \kappa) - (1 - m - s)\log(1 - m - s) + (1 - m)\log(1 - m) + (1 - s + m)\log(1 + m - s) - 2\kappa\log(\kappa) - (1 - s + m - \kappa)\log(1 - s + m - \kappa).$$
(85)

In the large N limit, the main contribution to $\Omega_1^+(N, M, 2S, 2k)$ comes from the neighborhood of κ_1^+ that is determined by solving $\partial_{\kappa} f_1(m, \sigma, \kappa) = 0$. A direct computation leads to the expression

$$\kappa_1^+ = \frac{1+m}{2} 2 \frac{s}{1+m} \left(1 - \frac{s}{1+m}\right). \tag{86}$$

Although Eq. (86) can be further simplified, it bears the following direct interpretation. In the thermodynamic limit, a configuration with magnetization M has $\frac{N+M}{2}$ up-spins. The probability that an up-spin is adjacent to a barrier is $\frac{s}{1+m}$; thus, the probability of being surrounded by a single barrier is $2\frac{s}{1+m}(1-\frac{s}{1+m})$, where the factor 2 accounts for the barrier being on either side.

It is also worth noting that, from the expressions of Eq. (82), we can determine the constraint

$$S \le \min\left(\frac{N-M}{2}, \frac{N+M}{2} - 1\right). \tag{87}$$

In the thermodynamic limit, this translates into $s \le 1 - |m|$.

In the following, let us proceed similarly to evaluate the enumeration of spins +1 adjacent to two barriers.

Enumeration of up-spins adjacent to two barriers

Proposition 3. The number $\Omega_2^+(N, M, 2S, k)$ of configurations of N spins, magnetization M, 2S defects and k up-spins adjacent to two barriers is

$$\Omega_{2}^{+}(N, M, 2S, k) = \begin{cases}
\frac{2N}{N-M} \binom{\frac{N-M}{2}}{N} & \text{if } k = S = \frac{N+M}{2}, \\
\frac{2N}{N-M} \binom{\frac{N-M}{2}}{S-k} \binom{\frac{N+M}{2}-S-1}{S-k-1} \binom{\frac{N-M}{2}+k-S}{k} & \text{otherwise}.
\end{cases}$$
(88)

As before, N and M must share the same parity. The number of spins +1 adjacent to two barriers may either be odd or even. From Eq. (88), we can obtain the exponential growth rate of $\Omega_2^+(N, M, 2S, k)$; it is given in the following proposition.

Proposition 4. Let us introduce the intensive (rescaled by N) variables:

$$m := \frac{M}{N}, \quad \kappa := \frac{k}{N}, \quad s := \frac{2S}{N}. \tag{89}$$

Then we have

$$\lim_{N \to +\infty} \frac{\log\left(\Omega_2^+(N, M, 2S, k)\right)}{N} = \frac{1}{2} f_2(m, s, \kappa),\tag{90}$$

where

$$f_2(m, s, \kappa) = (1 - m)\log(1 - m) - 2(s - 2\kappa)\log(s - 2\kappa) + (1 + m - s)\log(1 + m - s) + - (1 + m + 2\kappa - 2s)\log(1 + m + 2\kappa - 2s) - 2\kappa\log(2\kappa) - (1 - s - m)\log(1 - s - m).$$
(91)

At fixed m, σ , the function $f_2(m, s, \kappa)$ has a maximum at

$$\kappa_2^+ = \frac{1+m}{2} \left(\frac{s}{1+m}\right)^2. \tag{92}$$

Moreover, we note that $0 \le \kappa_2^+ \le 1/2$. The lower is attained when s = 0, corresponding to configurations with a sublinear number of barriers. The upper bound is reached when s = 1 and m = 0, which corresponds to configurations with an almost perfect alternation between spins +1 and spins -1.

Now we proceed with the enumeration of spins +1 adjacent to no barrier.

Enumeration of up-spins adjacent to no barrier

Proposition 5. The number $\Omega_0^+(N, M, s, k)$ of configurations of N spins, magnetization M, 2S defects and k up-spins (+1) adjacent to no barrier is

$$\Omega_{0}^{+}(N,M,2S,k) = \begin{cases} \frac{2N}{N-M} {N-M \choose \frac{N-M}{2}} & \text{if } S = \frac{N+M}{2} \text{ and } k = 0, \\ \frac{2N}{N-M} {S \choose 2} {N-M \choose 2} {N+M \choose 2} {N+M \choose 2} {N+M \choose 2} {N+M \choose 2} - S - k {N+M \choose 2} - S - k {N+M \choose 2} & \text{otherwise}. \end{cases}$$
(93)

In the large N limit, the asymptotic behavior of $\Omega_0^+(N, M, 2S, k)$ is provided by:

Proposition 6. Let us introduce the intensive (rescaled by N) variables:

$$m := \frac{M}{N}, \quad \kappa := \frac{k}{N}, \quad s := \frac{2S}{N}. \tag{94}$$

Then we have

$$\lim_{N \to +\infty} \frac{\log \left(\Omega_0^+(N, M, 2S, k)\right)}{N} = \frac{1}{2} f_0(m, s, \kappa), \tag{95}$$

where

$$f_0(m, s, \kappa) = (1 - m)\log(1 - m) - (1 - m - s)\log(1 - m - s) - 2(1 + m - s - 2\kappa)\log(1 + m - s - 2\kappa) + -(2s + 2\kappa - 1 - m)\log(2s + 2\kappa - 1 - m) + (1 + m - s)\log(1 + m - s) - 2\kappa\log(2\kappa).$$

$$(96)$$

For fixed m and s, the peak of the function $f_0(m, s, \kappa)$ is at

$$\kappa_3^+ = \frac{1+m}{2} \left(1 - \frac{s}{1+m}\right)^2. \tag{97}$$

Statistics for down-spins

To derive similar expressions for the enumeration of down-spins (-1) adjacent to one, two, or no barriers, we note that flipping all the spins in a configuration does not affect the number of defects, but reverses the magnetization. This observation enables us to obtain the following propositions.

Proposition 7. The number $\Omega_1^-(N, M, 2S, k)$ of configurations of N spins, magnetization M, 2S defects and 2k down-spins (-1) adjacent to a single barrier is:

$$\Omega_1^-(N, M, 2S, 2k) = \Omega_1^+(N, -M, 2S, 2k). \tag{98}$$

Proposition 8. The number $\Omega_1^-(N, M, 2S, k)$ of configurations of N spins, magnetization M, 2S defects and k down-spins (-1) adjacent to two barriers is:

$$\Omega_2^-(N, M, 2S, k) = \Omega_2^+(N, -M, 2S, k). \tag{99}$$

Proposition 9. The number $\Omega_0^-(N, M, 2S, k)$ of configurations of N spins, magnetization M, 2S defects and k down-spins (-1) adjacent to no barrier is:

$$\Omega_0^-(N, M, 2S, k) = \Omega_0^+(N, -M, 2S, k). \tag{100}$$

DERIVATION OF THE FOKKER-PLANCK EQUATION FROM THE MASTER EQUATION

In this section, we derive the Fokker-Planck equation associated to the Glauber dynamics of the Nagle-Kardar model. To this end, we consider the limit of large N and perform a Taylor expansion of the master equation Eq. (75) in terms of the rescaled variables m = M/N and s = 2S/N. Let us start with the term

$$A_{M+2\to M}^{2S\to 2S}B_1^+(N,M+2,2S)P_N(M+2,2S;t) - A_{M\to M-2}^{2S\to 2S}B_1^+(N,M,2S)P_N(M,2S;t); \tag{101}$$

for all the other terms of the master equation the procedure is the same. We thus use the following Taylor expansions:

$$P_N(M+2,2S;t) = p(m,s;t) + \partial_m p(m,s;t) \left(\frac{2}{N}\right) + \frac{1}{2} \frac{\partial^2}{\partial m^2} p(m,s;t) \left(\frac{2}{N}\right)^2 + O\left(\frac{1}{N^3}\right), \tag{102}$$

$$B_1^+(N, M+2, 2S) = \kappa_1^+(m, s) + \partial_m \kappa_1^+(m, s) \left(\frac{2}{N}\right) + \frac{1}{2} \frac{\partial^2}{\partial m^2} \kappa_1^+(m, s) \left(\frac{2}{N}\right)^2 + O\left(\frac{1}{N^3}\right), \tag{103}$$

$$A_{M+2\to M}^{2S\to 2S} = \frac{e^{-\beta[K(M+1)/N+h]}}{2\cosh\{\beta[K(M+1)/N+h]\}} = f_1^+(m) + \frac{\partial f_1^+(m)}{\partial m} \frac{1}{N} + \frac{1}{2} \frac{\partial^2 f_1^+(m)}{\partial m^2} \left(\frac{1}{N}\right)^2 + O\left(\frac{1}{N^3}\right), \tag{104}$$

$$A_{M \to M-2}^{2S \to 2S} = \frac{e^{-\beta [K(M-1)/N + h]}}{2 \cosh \{\beta [K(M-1)/N + h]\}} = f_1^+(m) - \frac{\partial f_1^+(m)}{\partial m} \frac{1}{N} + \frac{1}{2} \frac{\partial^2 f_1^+(m)}{\partial m^2} \left(\frac{1}{N}\right)^2 + O\left(\frac{1}{N^3}\right), \tag{105}$$

where

$$f_1^{\pm}(m) = \frac{e^{\mp \beta [Km+h]}}{2\cosh\{\beta [Km+h]\}}.$$
 (106)

Setting $\epsilon = 1/N$, we thus obtain (the dependence on m is omitted unless necessary):

$$A_{M+2\to M}^{2S\to 2S} B_{1}^{+}(N, M+2, 2S) P_{N}(M+2, 2S; t) = \kappa_{1}^{+} f_{1}^{+} p + \epsilon \left[2\kappa_{1}^{+} f_{1}^{+} \frac{\partial p}{\partial m} + \kappa_{1}^{+} \frac{\partial f_{1}^{+}}{\partial m} p + 2 \frac{\partial \kappa_{1}^{+}}{\partial m} f_{1}^{+} p \right] + \epsilon^{2} \left[2\kappa_{1}^{+} f_{1}^{+} \frac{\partial^{2} p}{\partial m^{2}} + 2\kappa_{1}^{+} \frac{\partial f_{1}^{+}}{\partial m} \frac{\partial p}{\partial m} + \frac{1}{2}\kappa_{1}^{+} \frac{\partial^{2} f_{1}^{+}}{\partial m^{2}} p + 4 \frac{\partial \kappa_{1}^{+}}{\partial m} f_{1}^{+} \frac{\partial p}{\partial m} + 2 \frac{\partial \kappa_{1}^{+}}{\partial m} \frac{\partial f_{1}^{+}}{\partial m} p + 2 \frac{\partial^{2} \kappa_{1}^{+}}{\partial m^{2}} f_{1}^{+} p \right],$$

$$(107)$$

and

$$A_{M \to M-2}^{2S \to 2S} B_1^+(N, M, 2S) P_N(M, 2S; t) = \kappa_1^+ \left[f_1^+ - \frac{\partial f_1^+}{\partial m} \epsilon + \frac{\epsilon^2}{2} \frac{\partial^2 f_1^+}{\partial m^2} \right] p. \tag{108}$$

From Eqs. (107)-(108) we deduce that

$$\begin{split} A_{M+2\to M}^{2S\to 2S} B_{1}^{+}(N,M+2,2S) P_{N}(M+2,2S;t) &- A_{M\to M-2}^{2S\to 2S} B_{1}^{+}(N,M,2S) P_{N}(M,2S;t) = \\ &= 2\epsilon \frac{\partial}{\partial m} (\kappa_{1}^{+} f_{1}^{+} p) + 2\epsilon^{2} f_{1}^{+} \frac{\partial^{2}}{\partial m^{2}} (\kappa_{1}^{+} p) + 2\epsilon^{2} \frac{\partial f_{1}^{+}}{\partial m} \frac{\partial}{\partial m} (\kappa_{1}^{+} p) = \\ &= 2\epsilon \frac{\partial}{\partial m} (\kappa_{1}^{+} f_{1}^{+} p) + 2\epsilon^{2} \frac{\partial}{\partial m} \left[f_{1}^{+} \frac{\partial}{\partial m} (\kappa_{1}^{+} p) \right]. \end{split} \tag{109}$$

Similarly, by symmetry, we have:

$$\begin{split} &A_{M-2\to M}^{2S\to 2S}B_{1}^{-}(N,M-2,2S)P_{N}(M-2,2S;t) - A_{M\to M+2}^{2S\to 2S}B_{1}^{-}(N,M,2S)P_{N}(M,2S;t) = \\ &= -2\epsilon\frac{\partial(\kappa_{1}^{-}f_{1}^{-}p)}{\partial m} + 2\epsilon^{2}\frac{\partial}{\partial m}\Big[f_{1}^{-}\frac{\partial}{\partial m}(\kappa_{1}^{-}p)\Big]. \end{split} \tag{110}$$

Using the procedure above, we also determine that

$$A_{M\pm2\to M}^{2S+2\to2S}B_{2}^{\pm}(N,M\pm2,2S+2)P_{N}(M\pm2,2S+2;t) - A_{M\to M\pm2}^{2S\to2S-2}B_{2}^{\pm}(N,M,2S)P_{N}(M,2S;t) = \\ = \pm2\epsilon\frac{\partial(f_{2}^{\pm}\kappa_{2}^{\pm}p)}{\partial m} + 2\epsilon\frac{\partial(f_{2}^{\pm}\kappa_{2}^{\pm}p)}{\partial s} + 2\epsilon^{2}\frac{\partial}{\partial m}\left[f_{2}^{\pm}\frac{\partial(\kappa_{2}^{\pm}p)}{\partial m}\right] + 2\epsilon^{2}f_{2}^{\pm}\frac{\partial^{2}(\kappa_{2}^{\pm}p)}{\partial s^{2}} \pm 2\epsilon^{2}\frac{\partial f_{2}^{\pm}}{\partial m}\frac{\partial(\kappa_{2}^{\pm}p)}{\partial s} \pm 4\epsilon^{2}f_{2}^{\pm}\frac{\partial^{2}(\kappa_{2}^{\pm}p)}{\partial m\partial s}$$
(111)

with the functions $f_2^{\pm}(m)$ given by

$$f_2^{\pm}(m) = \frac{e^{\mp\beta(Km+h\mp2J)}}{2\cosh[\beta(Km+h\mp2J)]},$$
(112)

and

$$A_{M\pm2\to M}^{2S-2\to 2S}B_0^{\pm}(N,M\pm2,2S-2)P_N(M\pm2,2S-2;t) - A_{M\to M\pm2}^{2S\to 2S+2}B_0^{\pm}(N,M,2S)P_N(M,2S;t) = \pm 2\epsilon \frac{\partial(\kappa_0^{\pm}f_0^{\pm}p)}{\partial m} - 2\epsilon \frac{\partial(\kappa_0^{\pm}f_0^{\pm}p)}{\partial s} + 2\epsilon^2 \frac{\partial}{\partial m} \left[f_0^{\pm} \frac{\partial(\kappa_0^{\pm}p)}{\partial m} \right] \mp 2\epsilon^2 \frac{\partial f_0^{+}}{\partial m} \frac{\partial(\kappa_0^{\pm}p)}{\partial s} + 2\epsilon^2 f_0^{\pm} \frac{\partial^2(\kappa_0^{\pm}p)}{\partial s^2} \mp 4\epsilon^2 f_0^{\pm} \frac{\partial^2(\kappa_0^{\pm}p)}{\partial s\partial m},$$
(113)

where

$$f_0^{\pm}(m) = \frac{e^{\pm \beta(Km + h \pm 2J)}}{2\cosh[\beta(Km + h \pm 2J)]}.$$
 (114)

In conclusion, gathering all the terms together, we obtain the Fokker-Planck equation for the Nagle-Kardar model:

$$\frac{\partial}{\partial t}p(m,s;t) = \frac{\partial}{\partial m}[D_1(m,s)p(m,s;t)] + \frac{\partial}{\partial s}[D_2(m,s)p(m,s;t)] + \\
+\epsilon \frac{\partial^2}{\partial m^2}[D_{mm}(m,s)p(m,s;t)] + \epsilon \frac{\partial^2}{\partial s^2}[D_{ss}(m,s)p(m,s;t)] + 2\epsilon \frac{\partial^2}{\partial m\partial \sigma}[D_{ms}(m,s)p(m,s;t)],$$
(115)

where the drift terms are equal to

$$D_{1}(m,s) = m + c_{1} \tanh(x) + c_{2} \tanh(x_{-}) + c_{3} \tanh(x_{+}) + K\epsilon \left(\frac{c_{4}}{\cosh^{2}(x)} + \frac{c_{5}}{\cosh^{2}(x_{-})} + \frac{c_{6}}{\cosh^{2}(x_{+})}\right),$$

$$D_{2}(m,s) = 2s - 1 + c_{2} \tanh(x_{-}) - c_{3} \tanh(x_{+}) + K\epsilon \left(\frac{c_{5}}{\cosh^{2}(x_{-})} - \frac{c_{6}}{\cosh^{2}(x_{+})}\right),$$
(116)

while the diffusion terms are defined by

$$D_{mm}(m, s) = 1 - c_4 \tanh(x) - c_5 \tanh(x_-) - c_6 \tanh(x_+),$$

$$D_{ss}(m, s) = 1 + c_1 - c_5 \tanh(x_-) - c_6 \tanh(x_+),$$

$$D_{ms}(m, s) = -m - c_5 \tanh(x_-) + c_6 \tanh(x_+)$$
(117)

with x := h + Km and $x_{\pm} := x \pm 2J$. Finally, the coefficients c_i (i = 1, ..., 6) entering the drift and diffusion terms have the following expressions:

$$c_{1} = -2s\left(1 + \frac{s}{m^{2} - 1}\right), \qquad c_{4} = -2\frac{ms^{2}}{m^{2} - 1},$$

$$c_{2} = \frac{m - 1}{2} + s + \frac{s^{2}}{m^{2} - 1}, \qquad c_{5} = \frac{m - 1}{2} + s + \frac{ms^{2}}{m^{2} - 1},$$

$$c_{3} = -\frac{m + 1}{2} + s + \frac{s^{2}}{m^{2} - 1}, \qquad c_{6} = \frac{m + 1}{2} - s + \frac{ms^{2}}{m^{2} - 1}.$$

$$(118)$$

LANGEVIN EQUATION ASSOCIATED TO THE FOKKER-PLANCK EQUATION

We now provide the derivation of the Langevin equation corresponding to the two-dimensional Fokker-Planck equation of Eq. (115). The derivation is based on Ref. [65].

Let us consider a set of d stochastic variables $\{\xi_i\}_{i=1}^d$, and the following d-dimensional Langevin equation written in Ito convention:

$$\dot{\xi}_i = h_i(\{\xi_i\}, t) + \sqrt{2} \sum_{i=1}^d g_{ij}(\{\xi_i\}, t) \Gamma_j(t) \quad (i = 1, \dots, d).$$
(119)

In Eq. (119), h_i and g_{ij} are time-dependent functions of the random variables ξ_i , while $\Gamma_j(t)$ are Gaussian stochastic processes fulfilling the normalizations $\langle \Gamma_i(t) \rangle = 0$ and $\langle \Gamma_j(t) \Gamma_i(t') \rangle = \delta_{ij} \delta(t - t')$. Its corresponding Fokker-Planck equation is given by [65]

$$\frac{\partial p}{\partial t} = \mathcal{L}_{FP}[p] \quad \text{where} \quad \mathcal{L}_{FP} = -\sum_{i} \frac{\partial}{\partial x_{i}} D_{i}(\{x\}) + \sum_{i,j} \frac{\partial^{2}}{\partial x_{i} \partial x_{j}} D_{ij}(\{x\}), \tag{120}$$

with

$$D_i(\{x\}, t) = h_i(\{x\}, t) \quad \text{and} \quad D_{ij}(\{x\}, t) = \sum_k g_{ik}(\{x\}, t)g_{jk}(\{x\}, t).$$
(121)

Hence, a given Langevin equation uniquely determines an associated Fokker-Planck equation; however, the reverse is not generally true [65]. It follows that the drift terms of the Langevin equation corresponding to the Fokker-Planck equation Eq. (115) are given by

$$h_m(m, s) = -D_m(m, s)$$
 and $h_s(m, s) = -D_s(m, s)$. (122)

Instead, the coefficients g_{mm} , g_{ms} , g_{sm} and g_{ss} must obey the following relations:

$$\epsilon D_{mm} = g_{mm}^2 + g_{ms}^2
\epsilon D_{ss} = g_{ss}^2 + g_{sm}^2
\epsilon D_{sm} = g_{ss}g_{ms} + g_{sm}g_{mm}
\epsilon D_{ms} = g_{mm}g_{sm} + g_{ms}g_{ss}.$$
(123)

In Eq. (123) there are 4 unknowns but 3 independent equations. This leads us to set constraints when choosing the coefficients g_{ij} . To see this, let us introduce the diffusion matrix

$$D = \epsilon \begin{pmatrix} D_{mm} & D_{ms} \\ D_{sm} & D_{ss} \end{pmatrix}, \tag{124}$$

and seek for a matrix G such that $D = GG^T$. As there are fewer equations than unknowns, we assume G to be lower triangular:

$$G = \sqrt{\epsilon} \begin{pmatrix} g_{mm} & 0 \\ g_{sm} & g_{ss} \end{pmatrix}. \tag{125}$$

It follows that

$$D_{mm} = g_{mm}^{2},$$

$$D_{ss} = g_{sm}^{2} + g_{ss}^{2},$$

$$D_{sm} = D_{ms} = g_{mm}g_{sm}.$$
(126)

The solution to this system is:

$$g_{mm} = \sqrt{D_{mm}}, \quad g_{sm} = \frac{D_{sm}}{\sqrt{D_{mm}}}, \quad g_{ss} = \sqrt{D_{ss} - \frac{D_{sm}^2}{D_{mm}}}.$$
 (127)

It can be checked that $D_{mm} > 0$ and $D_{ss} - D_{sm}^2/D_{mm} > 0$, such that the Langevin equation associated to the Fokker-Planck equation Eq. (115) is provided by

$$\begin{pmatrix} \dot{\xi}_m \\ \dot{\xi}_s \end{pmatrix} = - \begin{pmatrix} D_{mm}(m,s) \\ D_{ss}(m,s) \end{pmatrix} + \sqrt{2\epsilon} \begin{pmatrix} \sqrt{D_{mm}} & 0 \\ \frac{D_{ms}}{\sqrt{D_{mm}}} & \sqrt{D_{ss} - \frac{D_{ms}^2}{D_{mm}}} \end{pmatrix} \begin{pmatrix} \Gamma_m \\ \Gamma_s \end{pmatrix}.$$
 (128)

- [2] A. Campa, T. Dauxois, and S. Ruffo, Phys. Rep. 480, 57 (2009).
- [3] A. Campa, T. Dauxois, D. Fanelli, and S. Ruffo, Physics of long-range interacting systems (OUP Oxford, 2014).
- [4] N. Defenu, T. Donner, T. Macrì, G. Pagano, S. Ruffo, and A. Trombettoni, Rev. Mod. Phys. 95, 035002 (2023).
- [5] Y. Levin, R. Pakter, F. B. Rizzato, T. N. Teles, and F. P. Benetti, Phys. Rep. 535, 1 (2014).
- [6] P.-H. Chavanis, Int. J. Mod. Phys. B 20, 3113 (2006).
- [7] F. Bouchet and A. Venaille, Phys. Rep. **515**, 227 (2012).
- [8] M. Lewin, J. Math. Phys. 63, 10.1063/5.0086835 (2022).
- [9] P. L. Krapivsky and K. Mallick, Phys. Rev. E 111, 064109 (2025).
- [10] G. A. Baker, Phys. Rev. 130, 1406 (1963).
- [11] J. F. Nagle, Phys. Rev. A 2, 2124 (1970).
- [12] M. Kardar, Phys. Rev. B 28, 244 (1983).
- [13] D. Mukamel, S. Ruffo, and N. Schreiber, Phys. Rev. Lett. 95, 240604 (2005).
- [14] M. Kaufman and M. Kardar, Phys. Rev. B 29, 5053 (1984).
- [15] D. Bollé, R. Heylen, and N. S. Skantzos, Phys. Rev. E 74, 056111 (2006).
- [16] D. Gatteschi and A. Vindigni, in Molecular Magnets: Physics and Applications (Springer, 2014) pp. 191–220.
- [17] S. Gupta, J. Phys. A: Math. Theor. **50**, 424001 (2017).
- [18] B. Blaß, H. Rieger, G. m. H. Roósz, and F. Iglói, Phys. Rev. Lett. 121, 095301 (2018).
- [19] D. Dantchev, N. S. Tonchev, and J. Rudnick, Symmetry 17, 22 (2024).
- [20] D. Dantchev, N. Tonchev, and J. Rudnick, Phys. Rev. E 110, L062104 (2024).
- [21] D. Dantchev, N. S. Tonchev, and J. Rudnick, Eur. Phys. J. Spec. Top. (2025).
- [22] J.-T. Yang and J.-X. Hou, Eur. Phys. J. B 95, 190 (2022).
- [23] A. Campa, G. Gori, V. Hovhannisyan, S. Ruffo, and A. Trombettoni, J. Phys. A: Math. Theor. 52, 344002 (2019).
- [24] A. Campa, V. Hovhannisyan, S. Ruffo, and A. Trombettoni, J. Phys. A: Math. Theor. 58, 035005 (2025).
- [25] P. C. Hohenberg and B. I. Halperin, Rev. Mod. Phys. 49, 435 (1977).
- [26] T. Schneider, E. Stoll, and K. Binder, Phys. Rev. Lett. 29, 1080 (1972).
- [27] F. Wang, N. Hatano, and M. Suzuki, J. Phys. A: Math. Gen. 28, 4543 (1995).
- [28] R. B. Griffiths, C.-Y. Weng, and J. S. Langer, Phys. Rev. 149, 301 (1966).
- [29] L. Colonna-Romano, H. Gould, and W. Klein, Phys. Rev. E 90, 042111 (2014).
- [30] R. Aiudi, R. Burioni, and A. Vezzani, Phys. Rev. B 107, 224204 (2023).
- [31] K. Kikuchi, M. Yoshida, T. Maekawa, and H. Watanabe, Chemical Physics Letters 185, 335 (1991).
- [32] K. Binder, D. W. Heermann, and K. Binder, Monte Carlo simulation in statistical physics, Vol. 8 (Springer, 1992).
- [33] D. Landau and K. Binder, A guide to Monte Carlo simulations in statistical physics (Cambridge university press, 2021).
- [34] The fact that the number of defects is even is the consequence of choosing periodic boundary conditions.
- [35] M. E. Fisher and M. N. Barber, Phys. Rev. Lett. 28, 1516 (1972).
- [36] M. N. Barber, in *Phase Transitions and Critical Phenomena*, Vol. 8, edited by C. Domb and J. L. Lebowitz (Academic, New York, 1983) pp. 145–266.
- [37] V. Privman, ed., Finite Size Scaling And Numerical Simulation Of Statistical Systems (World Scientific, Singapore, 1990).
- [38] S.-K. Ma, Modern Theory Of Critical Phenomena (Routledge, 2001).
- [39] R. S. Ellis, J. Machta, and P. T.-H. Otto, Ann. Appl. Probab. 20, 2118 (2010).
- [40] F. J. Wegner, Phys. Rev. B 5, 4529 (1972).
- [41] B. M. Gorman, P. A. Rikvold, and M. A. Novotny, Phys. Rev. E 49, 2711 (1994).
- [42] M. Antoni, S. Ruffo, and A. Torcini, EPL 66, 645 (2004).
- [43] P.-H. Chavanis, Astronomy & Astrophysics 432, 117 (2005).
- [44] See the SM where we report the detailed calculations of the results presented in the main text, including Refs. [61, 65].
- [45] H. Touchette, Phys. Rep. 478, 1 (2009).
- [46] The magnetization M takes values from -N to N, in steps of 2, while the defects number ranges from 2 to N |M|, also in steps of 2 (except when $M = \pm N$, for which there is no defect). Hence, it follows that $0 \le s \le 1 |m|$.
- [47] P. Gaspard, J. Stat. Mech. 2012, P08021 (2012).
- [48] R. J. Glauber, J. Math. Phys. 4, 294 (1963).
- [49] N. G. Van Kampen, Stochastic processes in physics and chemistry, Vol. 1 (Elsevier, 1992).
- [50] The factor $N^2/4$ arises because M and 2S increase in steps of 2.
- [51] T. Mori, S. Miyashita, and P. A. Rikvold, Phys. Rev. E 81, 011135 (2010).
- [52] Y. Ozeki and N. Ito, J. Phys. A: Math. Theor. 40, R149 (2007).
- [53] N. Goldenfeld, Lectures on Phase Transitions and the Renormalization Group (CRC Press (Taylor & Francis Group), 1992).
- [54] The value of the exponent β can be also obtained by developing Eq. (6) around m = 0 on the critical line.
- [55] J. Guckenheimer and P. Holmes, *Nonlinear oscillations, dynamical systems, and bifurcations of vector fields*, Vol. 42 (Springer Science & Business Media, 2013).
- [56] J. Lee and I. Seo, Probab. Theory Relat. Fields 182, 849 (2022).
- [57] The calculation of the prefactor in front of $e^{N\Delta U}$ would need a deeper analysis of both the drift and diffusion terms of the Langevin equation [56].
- [58] M. Mézard, G. Parisi, and M. A. Virasoro, *Spin glass theory and beyond: An Introduction to the Replica Method and Its Applications*, Vol. 9 (World Scientific Publishing Company, 1987).
- [59] M. Caruel and L. Truskinovsky, Rep. Prog. Phys. 81, 036602 (2018).
- [60] A. Di Biasio, E. Agliari, A. Barra, and R. Burioni, Theor. Chem. Acc. 131, 1104 (2012).

- [61] T. Antal, M. Droz, and Z. Rácz, J. Phys. A: Math. Gen. 37, 1465 (2004).
- [62] The rising factorial is also called the Pochhammer symbol.
- [63] M. Abramowitz and I. A. Stegun, *Handbook of mathematical functions: with formulas, graphs, and mathematical tables*, Vol. 55 (Courier Corporation, 1965).
- [64] M. Cvitković, A.-S. Smith, and J. Pande, J. Phys. A: Math. Theor. 50, 265206 (2017).
- [65] H. Risken, in The Fokker-Planck equation: methods of solution and applications (Springer, 1989) pp. 63–95.